SPATIAL-TEMPORAL VARIABILITY AND PROJECTED RAINFALL OVER RWANDA

SEBAZIGA NDAKIZE JOSEPH

College of science and technology

School of Science

Master of Science in Atmospheric and Climate Science

2018

SPATIAL-TEMPORAL VARIBILTY AND PROJECTED RAINFALL OVER RWANDA

By

SEBAZIGA Ndakize Joseph

Registration Number: 217290981

A dissertation submitted in partial fulfillment of the requirements for the degree of

MASTER OF SCIENCE IN ATMOSPHERIC AND CLIMATE SCIENCE

In the College of Science and Technology

Supervisors: **Prof. Bonfils SAFARI**

Co-supervisor: Dr. ASHER Siebert

August, 2018

Declaration

I declare that this Dissertation contains my own work except where specifically acknowledged

Joseph Ndakize SEBAZIGA
217290981

Signed………………………………………..

Date…………………………………………..

DEDICATION

This work is dedicated to my wife NYIRASHIMWE Solange, daughter SEBAZIGA Ishimwe Lucie, son SEBAZIGA Shema Joshua, my parents, brothers and sisters.

ACKNOWLEDGEMENT

I am highly grateful to Almighty God for giving me the strength to study throughout the entire length of this course at the University of Rwanda.

I would like to express my sincere thanks to my supervisors Prof. Bonfils SAFARI and Dr. Asher Siebert for their advice, guidance, support and encouragement during the research period.

I also express my thanks to the entire members of my family for their support, encouragement and prayers during the period of my study, may God bless you all.

I wish to extend my special thanks to the Government of Rwanda through Rwanda Meteorology Agency (Meteo Rwanda) for granting me a study leave and allowing me to pursue my study at the University of Rwanda. My wishes of thanks extended to the International Centre for Tropical Agriculture (CIAT-Rwanda) for awarding me the scholarship to pursue my Master of Science degree at the University of Rwanda; I pray that you may continue nurturing more talented young scientists in the Country

Last but not least, I extend my special gratitude all of my workmates from Meteo Rwanda as well as my classmates for their valuable inputs and positive criticism that improved the output of this study.

ABSTRACT

Rainfall variability has presented significant challenges to nations worldwide and especially developing countries including Rwanda. The main objective of this study is to determine the rainfall variability and projected change over Rwanda. Data employed in this study include observed rainfall datasets (ENACTS) from 1981 to 2017 obtained from Rwanda Meteorology Agency (Meteo Rwanda) and the Coordinated Regional Downscaling Experiment (CORDEX) model outputs obtained from the CORDEX Africa portal. The study utilized graphical and statistical methods to assess the trend in rainfall variability. To assess the skill of the models in simulating the climate of Rwanda, correlation, absolute mean error, index of agreement and rainfall climatology difference plots analysis were used. The data show that high rainfall are concentrated over the high land and southwestern parts which reduces toward the central parts while the low rainfall amount are observed in the Eastern part of the country during MAM and OND as well on annual time scale.

The trend results from graphical method indicate clear non-uniform rainfall variability over Rwanda. Results from statistical methods show that there is sufficient statistical evidence to conclude that there is a significant increasing rainfall trend over Northern part of the northern province and southern province while there is a non-significant decreasing rainfall trend over eastern, Kigali city, Northern and central western during MAM,OND and annual time scale. The results indicated a coefficient of variation ranging between 20 and 32% during MAM rain season, 18 to 37% during OND rain season and 14 to 31% on annual time scale. Furthermore, results indicate that the north eastern part of the country exhibits a more variable rainfall. The IPSL and CCCma models have revealed a better performance in simulating the of Rwanda during MAM and OND rain season respectively compared to the other models used in study. The projected rainfall change results indicated a projected decrease in rainfall of 5 to 6% over Nyamagabe and Rubavu while other stations will exhibit an increase in rainfall of 2 to 6 % and 1 to 5% under both RCP8.5 and RCP4.5 respectively during MAM rain season. A projected decrease in rainfall of 1 to 5% over Musanze, Nyamagabe, Rubona, Byimana, Kigali and Rubengera under both RCP8.5 and RCP4.5 respectively. Ngoma revealed a decreasing (increasing) rainfall of 1% under RCP8.5 (RCP4.5). Kayonza will exhibit an increasing rainfall of 5% under RCP8.5 and a decreasing rainfall of 2% under RCP4.5 while other stations will experience a projected increase in rainfall ranging from 1 to 5% will be experienced over Nyagatare, Gicumbi and Kamembe under both RCP 8.5 and RCP 4.5 respectively.

KEY WORS

Rainfall variability, rainfall trend, Climate, climate change, Climate projections, RCP scenarios and CORDEX

LIST OF SYMBOLS AND ACRONYMS

CanESM2: Canadian Earth System Model second generation

CCCma: Canadian Centre for Climate Modelling and Analysis,

CORDEX: Coordinated Regional Climate Downscaling Experiment

DMI: Dipole mode index

DRC: Democratic Republic of Congo

EC-EARTH: European center for Earth System Models

EEA: Equatorial Eastern Africa

ENACTS: Enhancing National Climate Services

ENSO: El Niño Southern Oscillation

GCMs: General Circulation Models

HadGEM2-ES : Hadley Global Environment Model 2 - Earth System

ICHEC: Irish Centre for High-End Computing

IOD: Indian Ocean Dipole

IPCC: inter-Governmental Panel on Climate Change

IPSL: Institute Pierre-Simon Laplace

IPSL-CM5A-LR: Institute Pierre-Simon Laplace Climate model5A low resolution

IRI: International Research Institute for Climate and Society

ITCZ: Inter-Tropical Convergence Zone

MAM: March to May

MIROC: The Model for Interdisciplinary Research on Climate

MIROC5: Model for Interdisciplinary Research On Climate

MJO: Madden-Julian Oscillation

MOHC: The Met Office Hadley Centre MOH

MPI: Max-Planck-Institute

MPI-ESM-LR: Max-Planck-Institute EARTHE System Model low resolution

NE: North East

NH: Northern Hemisphere

NHS: Northern Hemisphere Spring

OLR: Outgoing Long wave Radiation

OND: October to December

QBO: Quasi-Biennial Oscillation

RCM: Regional Climate Model

RCPs: Representative Concentration Pathways

RMM1: Real-time Multivariate MJO principal component 1

RMM2: Real-time Multivariate MJO principal component 2

SE: South East

SH: Southern Hemisphere

SOI: Southern Oscillation Index

SON: September to November

S^t: Saint

TABLE OF CONTENT

LIST OF TABLES

LIST OF FIGURES

CHAPTER ONE

1.1 INTRODUCTION

Rwanda experienced wetter conditions over south-western and northern highlands regions while warmer condition was experienced over the central plateau and the eastern lowlands [1][2]. In Rwanda, annual rainfall varies geographically across the country due to the complex topography[3].

Over the past, Rwanda has experienced several weather related disasters attributed to space and time rainfall variability, including flash flood, prolonged wet spells, inundation, strong winds, convective rainfall and land slide among others. In the May, 1988 the northern, western and southern parts of the country, rainfall lead to 48 deaths, 1125 houses destroyed. In the November 2000, Karambo and Nyundo in Rubavu district registered over 200 houses damaged. In September 2001, 12 deaths, over 100 houses, 60 schools and crops damaged were recorded in southern, northern and western regions of the country. In the May 2002, 69 deaths were recorded in western, northern and Kigali, in the September 2005, 35 deaths and 379 houses destruction were registered in the western and northern regions. In September 2012, 19 deaths, 593 houses and 183 ha of land were destroyed. In 2013 15 deaths, 411 ha of land and 193 houses were affected [4]. In the years 2001, 2002, 2007, 2008 and 2012, devastating landslides and floods caused by heavy rainfall has been observed over the Northern (Gakenke, Cyeru, Rulindo and Gicumbi) and Western (Nyamasheke, Nyamagabe, Karongi and Ngororero) regions [4][5].

The flood hazard assessment based on a 25-year return period revealed that floods are prone in areas around the five catchments namely Nyabarongo, Sebeya, Nyabisindu, Mukungwa, and Kagitumba. In addition, based on historical flood events data, it was also indicated that flood hazards are likely to occur in many different locations in the country [4]. It was noted that torrential rainfall that occurs every year in Rwanda disturbs the circulation for many days, causes losses of people and damages the houses. While all districts are affected by heavy rain and related phenomenon, the highest costs of such events are observed the in mountains districts[6]. The analysis of temperature on annual time scale has indicated an abrupt change of temperature indicating that the climate of Rwanda was really changing[7].

1.2 Statement of the Problem

Rainfall is the most important weather parameter that affects socio-economic activities over Rwanda. Seasonality of precipitation is of critical importance to the many African stakeholders who depend upon the seasonal rains for agricultural and domestic purposes[8]. Changes in climate baseline, variability, and extremes will exceed the consequences on agricultural production, posing additional challenges on agricultural production and food security for a growing world population[9][10]. However, few studies on related subject have been carried out, leaving the gap on the understanding of rainfall variability and its projected change using CORDEX models. For that reason, studying the rainfall variability both in space and in time, their corresponding trend and rainfall projected change in Rwanda are needed.

1.3 Objectives

The main objective of this study was to determine the rainfall variability and projected change in Rwanda. To achieve the main objective, the following specific objectives were pursued:

1. To determine the spatial-temporal variability of rainfall during rain seasons and annual time scale over Rwanda.

2. To assess the performance of CORDEX models to simulate the climate of Rwanda

3. To determine the projected rainfall change over Rwanda.

1.4 Hypothesis of the Study

Temporal variability of the rainfall over Rwanda has resulted in extreme events such as the floods and frequent droughts that have far reaching socio-economic impacts to the country. Research has indicated that warm SSTs in central Indian ocean are thought to be responsible for the recent droughts in equatorial and subtropical Eastern Africa during the 1980s to the 2000s [11]. Over Rwanda, there is a significant rainfall variability and change which would cause severe floods and droughts.

1.5 Justification of the problem

Climate variability and change are threats to farmers because crop and animal production directly rely on rainfall [12]. Information on rainfall variability and change is important to ensure food security of the country that depends on the rain-fed agriculture. In addition, one of the factors that contribute to increased vulnerability of communities is lack of sufficient information on the spatial-temporal variability of rainfall on seasonal scale. It is expected that this study will fill the gaps by increasing the knowledge on the rainfall variability, trend and projected rainfall change over Rwanda and the results will serve as basis for future planning and decision making as well as development and management of agricultural, water resources and other rainfall-dependent sectors of the economy.

1.6 Area of Study

Rwanda is a landlocked country located in Central and Eastern Africa, bordered by the Democratic Republic of Congo (DRC) to the West, Uganda to the North, Tanzania to the East and Burundi to the South. Rwanda covers an area of 26,338 km^2 and lies between 1°4′ and 2°51′ south, and 28°53′ and 30°53′ east [13] .

Rwanda has a modified humid climate including rain forest and Savannah. The central and eastern regions of the country are of semi-arid type being located in the rain shadow of the western highlands of Rwanda. The highest annual rainfall totals are observed in the Southwestern and the high elevated Northwestern regions of the country [14]. The country experiences two rain seasons in a year, March to May being the long rain season (commonly known as 'Itumba') and the period from September to December being the short rain season (commonly known as 'Umuhindo'). A short dry season occurs from January to February (commonly known as 'Urugaryi') and a long dry season from June to August commonly known as 'Impeshyi')[15][16]. During the period of March to May (MAM) referred to as long rain season, Inter tropical convergence zone (ITCZ) moves from south to the north while during the September to December (SOND) referred to as short rain season, ITCZ moves from north to the south[7]

Rwanda comprises of five climate zones ranging from east to west. The eastern region bordering Tanzania falls in East Rwandan dry and hot lowland climate zone. The temperate climate zone of the central highlands with an elevation increasing from east to west separates the East Rwandan dry and hot lowland climate zone with the mountain climate. This climate exhibits a less temperature fluctuation than the East Rwandan dry and hot lowland climate zone. The mountain climate zone is situated over the Congo-Nile watershed and the volcanic chain of the Virunga in the north region of the country. The fourth climate zones in Rwanda is the Lake Kivu climate zone located in the lee of the Virunga volcano extending to Bugarama located in the southern part Lake Kivu[17]. The fifth climate zone is the north-Rwanda dry mountain climate zone located in the north western part of the volcanic region. The highlands regions (regions including volcanic chains of Virunga and the Congo-Nile ridge) receive an annual rainfall varying between 1300 and 1550 mm. The central plateau region receives an annual rainfall ranging between 1100 and 1300 mm. The regions around Lake Kivu and Bugarama plains receive an annual rainfall ranging between 1200 and 1500 mm while the Eastern lowlands receive an annual rainfall ranging between 700 and 1100 mm [18][2]. The study area is represented in **Figure 1**

The main factors that influence rainfall over Rwanda include: The Inter-Tropical Convergence Zone (ITCZ), Sub-tropical Anticyclones, Tropical Cyclones, Congo air mass and Global tele-connections and local systems.

1.6.1 Inter-tropical Convergence Zone (ITCZ)

Inter-tropical Convergence Zone (ITCZ) is formed by the rising air motion at the region of convergence because of the pattern of seasonal heating. Over East Africa, ITCZ is comprised of both the meridional arm formed by the convergence of easterly winds from the Indian Ocean and moist westerlies from the Atlantic Ocean and the Congo Basin and zonal arms formed by the convergence of Southeasterly and Northeasterly trade winds and these are responsible for both the long and short rainfall seasons when ITCZ is close to the equator[19].

Rainfall patterns during March to May (long rains) and September to December (short rains) over East Africa where Rwanda is located are largely controlled by movement of the intertropical convergence zone (ITCZ) which makes the variability of the respective rains to be associated with sea surface temperature (SST) patterns over the Atlantic and Indian oceans and the convergence of Saint Helena Anticyclones from the South Atlantic Ocean and Mascarene Anticyclones from the Indian Ocean[20][13][21]. The short rains occur when the overhead sun starts to move from the Northern Hemisphere towards the equator with the ITCZ lagging behind for a longer period. This is because the large landmass in the Northern Hemisphere takes longer to cool while the large oceans around the Equator take longer to heat[19].

1.6.2 Monsoons

Two distinct monsoons are observed over the equatorial eastern Africa (EEA) region. These are the northeast (NE) monsoons during December to February and southeast (SE) monsoons during June to August and a transition occurs from the NE to SE monsoons during the period of the Northern Hemisphere Spring (NHS) season during March to May characterized by convergence, in the EEA region, of low-level equatorward moving air masses from both hemispheres which constitute the monsoonal flows and the zone of convergence is the ITCZ [22]. Analysis of the individual wettest or driest years showed that before the start of the EEA long-rains season, easterlies are dominant near the Equator and westerlies near 15°S in the lower troposphere, while at the end of the rain season the westerlies are located to the north of the Equator, near 5°N, with easterlies on their lateral sides. However, during the EEA long-rains season westerly and easterly wind events occurred in alternation over the EEA region[22].

1.6.3 EL-Niño Southern Oscillation (ENSO)

EL-Niño is the anomalous warming of central and eastern equatorial Pacific Ocean where sea surface temperature anomalies are of magnitudes greater than 0.5^{0}C. If this anomalous condition persists for five or more months, the condition is termed as an EL-Niño episode[23]. There is a strong relationship between rainfall over East Africa and the evolutionary phase of ENSO[24][25] [26][27]. Over East Africa, EL-Niño increases probability of being unusually wet during OND while MAM remains largely unaffected[28][29]. the wetter (drier) conditions were linked to El Niño (La Nina) events [18][27] [30][31]. During the El Niño events, increased atmospheric moisture and the resultant heavy rainfall are due to high evaporation rate while during La Nina events the opposite is correct[30][32][33]. It was noted that although there were some relationships between the Southern Oscillation and seasonal rainfall over parts of East Africa, some of the extreme wet and dry episodes were not related to the Southern Oscillation[34]. Over Rwanda, there is a relationship between ENSO and rainfall patterns where El Nino is link with positive anomalies (wet years) while La Nina shown a correspondence with negative anomalies (dry years) [16][18] the normal years were largely linked with negative (positive) long (short) rains anomalies while the occurrence of El Niño and La Niña events in the same year does not show a clear association with rainfall anomalies[16].

1.6.4 Quasi-Biennial Oscillation (QBO)

This is the alternation of zonal winds (westerly and easterly wind) regimes in the lower stratosphere with a period of 26-30 months. According to the correlation analysis between the phases of the QBO and Kenyan rainfall, the westerly phase of the QBO is accompanied by increased rainfall while the easterly phase is accompanied by decreased rainfall [35]. The relationship between March to May seasonal rainfall anomalies over Eastern Africa and the lower equatorial stratospheric zonal wind from 1964 – 1995 at an inter-annual timescale has shown that there is a significant positive simultaneous and non-zero lag correlations between March to May seasonal rainfall anomalies and QBO over East Africa, with higher correlations over the western regions of Eastern Africa while December to February season was observed to have the weakest relationship[36].

1.6.5 Indian Ocean Dipole (IOD)

Indian Ocean Dipole (IOD) refers to the difference between the sea surface temperature anomalies of the western and south eastern equatorial Indian Ocean[37]. The anomalous warm SSTs (positive phase of the IOD) are sometimes experienced over western Indian Ocean and cold SSTs (negative phase of the IOD) over the eastern region resulting in rainfall over East Africa since moisture is pushed into the region thus activating atmospheric convection and leads to enhanced rainfall during the rainy season and wet spells during the dry season while the negative phase involves high SSTs over the eastern Indian Ocean and cold SSTs over the western Indian Ocean which does not enhance rainfall over East Africa[37].

1.6.6 Sub-tropical Anticyclones

Sub-tropical anticyclones are quasi-permanent high pressure cells characterized by anticyclonic circulation which gives rise to subsidence and low level horizontal velocity divergence of air masses. The four major anticyclones, which influence the flow of winds over the region are; the St. Helena high pressure system to the south west of Atlantic ocean, the Mascarene high pressure system to south west Indian ocean, the Arabian high in the middle east and Azores high pressure system.

The position and intensity of anticyclones such as Saint Helena, Mascarenes, Siberian and Azores control the rainfall seasons over Rwanda [20][13][21]. The Mascarene anticyclones from the coast of Mozambique in the Indian Ocean which converges with wet winds from Saint Helena anticyclones which forms from the South Atlantic Ocean that passes over the Congo basin and Lake Kivu to form the ITCZ affects the rainfall season over Rwanda. These anticyclones are responsible for the heavy rainfall between March and May. During the long dry season (June to August), Rwanda is influenced by the dry Saint Helena and Azores anticyclones which cause the dry conditions over the county [20][13][21][38][39]. During the month of September, the ITCZ starts at the Somalian coast and passes over Lake Victoria where it gets humidity and brings rain to Rwanda , before heading southwards by the end of November. During December to February, winter monsoon push dry and cold air masses from the Arabian Sea over Lake Victoria to gather humidity, which gives a little rainfall in the highlands region of the country[32][20][27] [13][21][38][39].

1.6.8 Madden–Julian Oscillation (MJO)

The study conducted over the eastern African has indicated that intra-seasonal wet events in East Africa are embedded in large-scale zonal circulation anomaly patterns along the equator, showing distinct eastward propagation where wet events display a clear phasing with respect to the MJO cycle expressed as out-of-phase variations between the west (Highland) and the east (coastal) areas and suggested to reflect different rain-causing mechanisms[40].

MJO phases leading to wet spells in the western region are those associated with the development of large-scale convection in the Africa-Indian Ocean region and unambiguously related to deep convection, enhanced by low-level westerly moisture advection while MJO phases leading to wet spells in the eastern region are often those associated with overall suppressed deep convection in the Africa/Indian Ocean region and the contrasting rainfall conditions found in the two regions for the two opposite MJO phases are strongly correlated with the pressure gradient between the Indian and Atlantic Oceans [40]. The study associating the MJO and wet and dry spell over Rwanda has indicated a moderate degree of association between MJO indices and rainfall over Rwanda where the highest variance of daily rainfall explainable by Real-time Multivariate MJO principal component 2 (RMM2) indices is 25% while Real-time Multivariate MJO principal component 1 (RMM1) indices could explain 16.8% [41].

1.6.9 Local Systems

The influence of topography on east African climate was investigated using the International Centre for Theoretical Physics Regional Climate Model, with focus on October to December season, has indicated that the mean rainfall significantly reduces while the mean temperature significantly increases over the region when topography elevation is reduced[42]. Based on the model, the topography was reduced to 25%, resulting in the mean rainfall reduction by about 19% and the mean temperature increase of about 1.4°C over east Africa[42]. The study of the impacts of topography on spatial and temporal rainfall distribution over Rwanda based on WRF model indicated that topography leads to a decrease in rainfall amounts in both MAM and SOND seasons with varying magnitudes[3]. It was also noted that over Rwanda, rainfall is concentrated over highlands hence the influence of orography is very strong[14].

CHAPTER TWO

2.0 LITERATURE REVIEW

2.1 Climate variability

Rainfall is very important weather and climate parameter that influence economic activities in East Africa as well as Rwanda. Rainfall is a climatic parameter which present a largest time and space variability over the tropical region [43]. The systems that influence rainfall over East Africa region are sometimes linked with too much or failure of rainfall resulting to floods or droughts[44]. It is important to note that the performance of a given rainy season does not only depend only on rainfall total amount, but an adequate distribution of the rains throughout the year is also requires especially in the regions where they normally receive small amount of rains fall within a limited period of time. The failure in rainfall may ranges from late onset, earlier cessation of rainfall or short but intense rainfall events separated by long dry spells[44].

Most of East Africa region where Rwanda is located, experiences bimodal rainfall[45] which is associated with the north-south and south-north movement of the ITCZ [46]. Rainfall frequency and intensity variability has been observed with Africa being the most affected during the past century[47] [48][49][50] where sub-Saharan Africa has become more arid [51][52][53]. Recent studies suggest the potential for increased inter-annual variability in East African rainfall under future climate conditions, although the degree of inter-model agreement is very low for the region and the local variability from this coupled climate model is a distinct annual cycle of rainfall occurring with double peaks in long season (MAM) and short season (OND)[54].

Other studies have shown that spatial variability of short rains is coherent and shows strong connections with large-scale circulation over the Pacific and Indian oceans and the strong ridging from the south in the lower levels indicates that easterly anomalies were associated with a significant reduction of rainfall over the East Africa[55]. A study conducted over the eastern Africa has indicated that during long rain, the western parts of the region tend to be associated with an anomalous westerly component of the wind and anomalous convergence, although the long rains period coincides with a marked easterly component of the wind over the eastern region of East Africa where most of the rain days occur with a significant reduction of this component, or even its inversion [45].

East Africa experiences the dipole rainfall pattern that is characterized by increases over the northern region and decreases over the eastern and southern regions[32][20] [30][18]. The pattern in SST anomalies manifested during the IOD events has strong signals on the regional climate system during the OND rainfall season, the study has demonstrated that some of the extreme rainfall conditions over East Africa were associated with positive and negative IOD phases, with a strong linkage during El Niño/La Niña years[56].

The study of the East African rainfall variability associated with the Madden-Julian Oscillation(MJO), revealed a strong association between East African rainfall and MJO to the west of the region [22][57]. It was further noted than in the tropics, where the fluctuations in land surface temperatures are small, OLR reflects variations in cloudness or rainfall and can be used as proxy of convection that capture convectively driven MJO along the equator[58]. The study on the influence of the Madden–Julian Oscillation on East African Rainfall shown that low-level westerly wind anomalies are seen to accompany wet events in the west and easterly ones in the east, which indicates that the latter has a major influence on rainfall at the daily time-scale while lower air temperatures in the upper troposphere were observed during the MJO cycles that present the highest common variance with East African rainfall [40].

Further research has indicated that warm SSTs over the Indian ocean are thought to be responsible for the recent droughts in equatorial and subtropical Eastern Africa during the 1980s to the 2000s [11]. It was also indicated that over much of Kenya, Uganda, Rwanda, Burundi and southern Somalia, there are signals of an increasing trend in rainfall under global warming where wet extremes are projected to increase during both MAM and OND rain seasons[59].

It was also noted that over Rwanda, April and November are the monthly rainfall peak for MAM and SOND and more rainfall is received during MAM compared to SOND seasons concentrated over highlands hence the influence of orography is very strong over Rwanda[3][14]. The composited wind patterns for wet events indicated the presence of strong low level convergence accompanied with enhanced upper level divergence while SST composites shown that wet events over Rwanda are marked by cooler Atlantic Ocean and warmer Indian ocean. However, during the dry events, the Atlantic was warm while the Indian ocean was cooler [14]. High frequency of rain days over Rwanda usually occur between the third week of March and the second week of May over western part, April to the second week of May over central and eastern part, third week of March to third week of May over northern part [41]. The climate variability of Rwanda is one of the most significant factors influencing year to year crop production, water regime of fields and wetlands are closely linked to rainfall and could be one of the limiting constraints for crop production and food security. Lights winds were observed around the year with a modal wind speed in the 2–4ms^{-1} range. The highest wind speeds was observed to be around 11ms^{-1} during the rain seasons and the wind directions have a clear seasonal shift, with Easterlies and North-East winds dominate the short dry season while Southerlies and South Westerlies dominate the long rain season[60].

2.2 Climate projection

Over the recent past decades, changes in climate have caused impacts on natural and human systems on all continents which indicated the sensitivity of natural and human systems to changing climate [61]. It is projected that extreme precipitation events will become more intense and frequent in many regions [61]. The projection rainfall over Rwanda is important as it helps in understanding the expected changes, with a view to predicting their impacts on expected changes and variability. It was indicated that the climate change in Africa will have variable impacts on crops, with both production losses and gains possible [62]. Crop yields in Africa may fall by 10–20% to 2050 due to the warming and drying, but in some regions yield losses may be much more severe, where as in other regions crop yields may increase [63].
The Fourth Assessment Report of the Intergovernmental Panel on Climate Change (IPCC) predicts that climate change is likely to have a significant effect on agricultural production in many African countries [64] while the Fifth Assessment Report of the Intergovernmental Panel on Climate Change (IPCC_AR5) indicated a very likely decrease in annual observed rainfall over Africa over the past century in parts of the western and eastern Sahel region and a very likely increase in rainfall was observed over parts of eastern and southern Africa[65]. Over the eastern Africa, models suggest that rapid warming of the Indian Ocean may be the cause of decrease in rainfall over the region during long rain season (March to May) in the last decades[65]. According to the IPCC projection, a likely increase in annual average rainfall is projected over the areas of central and eastern Africa[65].

Rwanda, being a rain fed agricultural country; it may be subject to different effects of climate change, convective instability, associated with surface heating of the moist air, combined with orographic uplift, produces frequent convective precipitation events that are often associated with intense rainfall, lightning, hail, and damaging winds. This may be associated with frequently observed Partners over the western and northern highland of Rwanda where they receive intense rainfall, lightning, hail while the low land of the eastern part of the country are mainly subject to damaging winds. A critical first step in conducting climate change assessments is obtaining projected future climate data. This data may be obtained from the General Circulation Models (GCMs) which are used to project future climate, due to their large map grid cells, studies which examine a specific point on the globe, require the individual to conduct a site assessment to scale the larger GCM output down to a specific point [66].

To obtain precipitation projections from GCM for use in localized impact studies, the combined spatial and temporal downscaling techniques are recommended [66]. Downscaling is a quantitative method which involves regressing modeled synoptic-scale atmospheric trends to observed micro-scale localized weather to determine correlations which are then applied to modeled synoptic-scale of localized weather [67].

Due to the fact that the time and computing power requirements for learning and applying downscaling methods can be discouraging, a rapid method of obtaining downscaled future climate data using models which are already globally validated with observed datasets has greatly expanded the availability of such data to scientists and policy planners interested in conducting future climate impact analyses [68]. Based on the assumption that local climate is a combination of large-scale atmospheric characteristics and local-scale features, numerous techniques have been developed to provide climate change information at scales more relevant to decision makers. However, this information contains uncertainties inherent in the prediction process and some uncertainties in the climate modeling process are not reducible. But at the same time, perfect information is not necessary for improved decision making. The users must account for these uncertainties in the application of the information [69]. Studies at fine spatial scales are needed to resolve local climate change hot spots within regions [9] and forms the basis of a community-led solution that is ideal for smallholder farmers [70].

Downscaling can be performed on both spatial and temporal time scale. Spatial downscaling refers to the methods used to derive finer-resolution spatial climate information from GCM output while temporal downscaling refers to the derivation of fine-scale temporal information from coarser-scale temporal GCM output [69]. Dynamical downscaling relies on the use of a regional climate model (RCM), similar to a GCM in its principles but with high resolution by incorporating the GCM specified boundary conditions., more complex topography, the land-sea contrast, surface heterogeneities, and detailed descriptions of physical processes in order to generate realistic climate information at a spatial resolution of approximately 20–50 kilometers while statistical methods can provide station-scale climate information which makes it viable and advantageous for institutions that do not have the computational capacity and technical expertise required for dynamical downscaling [69]. More information on RCMs can be found in [69]. Statistical downscaling involves the establishment of empirical relationships between historical and/or current large-scale atmospheric and local climate variables. It is based on the assumptions that there is a strong relationship between the predictor and predictand; the statistical relationship between the predictor and predictand does not change over time; the predictor carries the climate change signal and GCMs accurately simulate the predictor [69]. However, this approach relies on the critical assumption that the relationship between present large-scale circulation and local climate remains valid under different forcing conditions of possible future climates [71]. It was shown that significant biases in individual model depends on sub-region and season; however, the ensemble mean has better agreement with observation than individual models [72]. In general, multimodel ensemble mean simulates eastern Africa rainfall adequately and can therefore be used for the assessment of future climate projections for the region [72]. However, a study conducted over the east Africa indicated that an observed drying trend and projected increase in rainfall has placed this region in an apparent climate paradox [73]. It was further noted that the recent regional scale drying trend in East Africa was dominated by an abrupt decline in long rain season around 1998–1999 and associated with a shift of Pacific decadal variability to its cold phase[73]. Furthermore, the same study indicated a possibility that a warming trend in the western tropical Pacific contributed to the severity of recent droughts, the timing of the recent decline is closely tied to Pacific decadal variability[73]. Over the eastern Africa, an apparent climate paradox is seen to result from a mismatch of timescales on one hand (recent drying versus long-term wetting) and from taking climate change projections at face value on the other[73]. The inability of coupled models to capture fundamental aspects of the current climate undermines confidence in the future climate projections in East Africa. Given substantial errors in coupled climate models' ability to simulate the current climate, it remains an open question as to whether or not the future climate in East Africa will become wetter[73].

Due to that dynamical downscaling is computationally expensive, many collaboration projects are generating climate simulation from dynamical downscaling for model inter-comparisons and impact assessments. These projects include the Coordinated Regional Climate Downscaling Experiment (CORDEX) produces dynamical downscaled climate simulation for all continents

[74]. It should be further noted that all CORDEX RCMs are set to 0.44˚ by 0.44˚ spatial resolutions corresponding to 50 km by 50 km [75]. The study using RCMs from CORDEX to simulating rainfall characteristics over Mbarali River Catchment in the Rufiji Basin, Tanzania, has indicated a better performance to reproduce the rainfall characteristics and the ensemble average performed better than individual models in representing rainfall [76]. The evaluation of the performance of RCMs from CORDEX to simulate rainfall over Tanzania has indicated that RCMs capture the annual cycle of rainfall well, however under estimate and overestimate the amount of rainfall during MAM and OND seasons respectively and most RCMs reproduce interannual variations rainfall[75].

The evaluation of the ability of CORDEX RCMs in simulating monthly rainfall variation during the austral summer half year (October to March) over southern Africa has indicated that a majority of the RCMs adequately capture the reference precipitation probability density functions, with a few showing a bias towards excessive light rainfall events[77]. It was found that most RCMs reasonably simulated the rainfall climatology over the three sub-regions and also reproduced the majority of the documented regional responses to ENSO and IOD forcings. At the same time, it was shown that significant biases in individual models depend on sub-region and season; however, the ensemble mean has better agreement with observation than individual models[72]. The CORDEX RCMS do well retrospectively with past years does not mean that they will necessarily capture the behavior of the future as well as they have captured the behavior of the past. In general, it was found that the multimodel ensemble mean simulates eastern Africa rainfall adequately and can therefore be used for the assessment of future climate projections for the region[72].

CHAPTER THREE

3.0 DATA AND METHODOLOGY

3.1 Data

3.1.1. Station data

The observed rainfall datasets used in this study were collected from Rwanda Meteorology Agency (Meteo Rwanda). The dataset were developed by Meteo Rwanda in partnership with International Research Institute for Climate and Society (IRI) and the data set is commonly known as the Enhancing National Climate Services (ENACTS) data set. The spatial resolution of ENACTS is 0.0375 degrees (~4km) and 0.05 degrees (~5km) for rainfall and temperature respectively. It is important to note that the ENACTS gridded data covers the whole country but for the purpose of this study, the twelve Agro synoptic stations will be considered. The month of September, which is part of the short rains season in Rwanda, was not considered in this study due to the fact that the short rains in the former month do not correlate significantly with ENSO events while December showed a good relationship [32][20] [78]. The spatial distribution of the stations used under this study is presented in the **Figure 2.**

3.1.2 CORDEX models data

Coordinated Regional Downscaling Experiment (CORDEX) model outputs used in this study were obtained from the CORDEX Africa portal at a spatial resolution 0.44° by 0.44° corresponding to 50 km by 50 km resolution. The selected models have contributed to the Coupled Model Intercomparison Project phase five (CMIP5) in support of the Intergovernmental Panel on Climate Change (IPCC) Fifth Assessment Report (AR5). In this work, six CORDEX model were used and corresponding descriptions are provided in the **Table1.**

3.1.3 Representative Concentration Pathways

During this work two Representative Concentration Pathways (RCP4.5 and RCP8.5)[79] [80] have been selected for this work and the corresponding descriptions are provided in the **Table 2.**

3.2 Methodology

Spatial-temporal analysis and statistical performance measures were used to achieve the objective of this study.

3.2.1 Temporal and Spatial Analysis

Spatial-temporal analyses methods were used to achieve the first specific objective which is to determine the spatial-temporal variability of rainfall and their corresponding trend over Rwanda.

The temporal analysis of seasonal to annual rainfall consisted of determining the seasonal and annual rainfall climatology. Temporal variability of rainfall was investigated using a time series analysis where seasonal and annual climatology were computed and subjected to a time series analysis using Python tool.

3.2.1.1 Trend Analysis

A trend refers to long term movement of a time series [43]. There are several methods to describe trends in climatological data. These methods can be grouped into different categories, including: graphical, polynomial, and statistical methods. In present study, the trend analysis was established through a graphical plot while Statistical methods were used to test the statistical significance of the observed trends in a time series.

3.2.1.2 Graphical Method

The graphical method involves plotting seasonal rainfall from March to May (MAM), October to December (OND) and annual rainfall data against time. The advantage of this method is that it provides quick visual observation of the presence trend in a given time series. Moreover the use of the graphical approach for trend analysis is simple. On the other hand graphical methods has shortcoming such as its subjectivity as it depends on individual judgments and some data set are lost by some smoothing techniques[81].

3.2.1.3 Statistical Method

The visual method of determining trends from a graph is very subjective therefore statistical method can also be used. Statistical methods were used to test the statistical significance of the observed trends in a time series. A similar method has been applied by Okoola (2000) [82][43].

These methods are classified as parametric and non-Parametric tests. In the present study, the Mann–Kendall (MK), a nonparametric rank-based test used to determine the nature of the trend of a given time series [79][83][84][85]. The MK test has been used in many studies over East Africa [7] [86] [87][88]. Positive values denote an increasing trend whereas negative values denote a downward slope[79]. To estimate the magnitude of rainfall change, the Theil–Sen's slope estimator[89][90] was used. The statistical significance was reported on the basis of level of significance (p-value or alpha) of 0.05.

The Mann-Kendall [85] were calculated as follows:

$$S = \sum_{i=1}^{n-1} \sum_{j=i+1}^{n} sgn(x_j - x_i) \tag{1}$$

In Equation (1), n denotes the number of data points while x_i and x_j are the data values in the time series i and j, where $(j > i)$ respectively, and $sgn(x_j - x_i)$ is the sign function as:

$$sgn(x_j - x_i) = \begin{cases} +1 \;\; if \; (x_j - x_i) > 0 \\ 0 \;\; if \; (x_j - x_i) = 0 \\ -1 \;\; if \; (x_j - x_i) < 0 \end{cases} \tag{2}$$

The variance was computed using the Equation (3) as:

$$Var(S) = \frac{n(n-1)(2n+5) - \sum_{i=1}^{P} t_i(t_i-1)(2t_i+5)}{18} \tag{3}$$

The standard normal test statistic Z was computed using Equation (4) as follows:

$$Z = \begin{cases} \frac{S-1}{\sqrt{Var(s)}} & if\ S > 0 \\ 0 & if\ S = 0 \\ \frac{S+1}{\sqrt{Var(S)}} & if\ S < 0 \end{cases} \qquad (4)$$

3.2.1.4 Rainfall Variability and Reliability

In this study an attempt has been made to examine reliability and variability of seasonal and annual rainfall records. It involves both time and space variability, some methods that was used to examine rainfall variability and reliability include coefficient of variability and rainfall reliability. The Coefficient of Variability (CV) is a measure of degree of variability that is expressed as a percentage. The coefficient of variation (CV) is defined as the percentage ratio of the standard deviation (σ) to the mean( ).this method was also used by [82].

(4) CV= 100 X σ/X (5)

The reliability of seasonal and annual stations rainfall records were examined using method of coefficient of variation. High (low) coefficient of variability means a low (high) reliability of rainfall[82]. Reliability (R) is given by the formula;

R =100-CV (6)

Spatial map of seasonal and annual coefficient of variation was drawn using surfer software to show how the rainfall is distributed with space.

3.2.2 Assessing the performance of CORDEX models to simulate the climate of Rwanda

In this study, statistical measures were used to assess the performance of CORDEX to simulate the climate of Rwanda. CORDEX model rainfall and temperature datasets were obtained from the CORDEX Africa portal. Statistical measures were used to check the accuracy, bias, and reliability of the generated data compared to the observed rainfall from Meteo Rwanda data[91]. Comparison between rainfall data from CORDEX RCMs and observed rainfall from Meteo Rwanda were done to test the ability of the CORDEX to reproduce the seasonal total, annual cycles, interannual variability and annual total. Statistical measures used to test the CORDEX model performance include Mean absolute error (MAE), Pearson correlation coefficient(r) [91][92][93] and the index of agreement (d)[91].

3.2.2.1. Mean absolute error (MAE)

The mean absolute error (MAE) is the arithmetic average of absolute differences between the observed (Oi) and predicted (Pi) values[91]. It is expressed as:

$$MAE = \frac{1}{n}\left[\sum_{i=1}^{n} |Pi - Oi|\right] \qquad (7)$$

For perfect prediction, the MAE ranges between zero and large positive values, but a perfect MAE is zero [91]. It has been indicated that MAE is a more natural measure of average error unlike RMSE which is unambiguous and tends to over-emphasize the impact of large errors in individual years or locations and it recommended that the evaluation and inter-comparisons of average model-performance error should be based on MAE.[94][95][96].

3.2.2.2. The correlation coefficient(r)

The correlation coefficient(r) was used to measure the level of association between the observed values and the model outputs. A correlation coefficient of 1 denotes positive linear relation while correlation coefficient of -1 denotes a negative linear relationship in the observed and model outputs values. A correlation coefficient equal to 0.0 represents no association between the two variables the observed values and the model outputs. Correlation coefficient(r) was also used by[97].

$$r = \frac{\frac{1}{n}\sum_{t=1}^{n}(Oi-o)(Pi-p)}{\sqrt{\frac{1}{n}\left[\sum_{t=1}^{n}(Oi-o)^2\right]\left[\sum_{t=1}^{n}(Pi-p)^2\right]}} \qquad (8)$$

3.2.2.3. Index of agreement (d)

The index of agreement (d) is the ratio of the mean square error and the potential error multiplied by number of observation and then subtracted from one and is given by [91]:

$$\mathrm{d} = 1 - \left[\frac{\sum_{i=1}^{n}(Pi-Oi)^2}{\sum_{i=1}^{n}(|Pi-p|+|Oi-o|)^2}\right] \qquad (9)$$

Where n is the total number of observations, Pi is the predicted value, Oi is the observed value, and p and o are the means of the predicted and observed values, respectively.

The relative accuracy measure 'd' accounts for the differences between means and variances of Pi and Oi. It ranges between 0.0 and 1. Values close to 1 indicates better agreement between the Oi and Pi [93][91].

3.2.3 Rainfall projection

To achieve the third specific objective which is to determine the projected change in rainfall over Rwanda, the IPSL and CCCma CORDEX models have revealed a better performance during the March to May and October to December rainfall season respectively compared to the other six CORDEX models used under this study. For this reasons, IPSL and CCCma CORDEX models were considered in the next sections in projecting rainfall using the RCP 4.5 and RCP8.5. Temporal variability of projected rainfall was investigated using a time series analysis whereas spatial variability of rainfall was analyzed and plotted using Surfer that provided spatial maps. The trend in projected rainfall analyzed using the Mann–Kendall (MK [83][84].

In order to downscale our results, a simple linear regression were developed which estimates the intercept and slope of a linear model which predicts the value of a single dependent variable (y) against a single independent variable (x) in the form [98][99]

$$y = a + bx \qquad (10)$$

Where a is the intercept of the straight line (the value of y when it crosses the Y-axis) while b is its slope.

CHAPTER FOUR

4.0 RESULTS AND DISCUSSION

This chapter summarizes the results obtained from the various methods used to achieve the specific objectives of the study. The results include observed spatial and temporal patterns of rainfall, skill of CORDEX models in simulating observed rainfall and the projected rainfall change from CORDEX models.

The spatio-temporal variability of rainfall during March to May (MAM) and October to December (OND) rain seasons and annual timescale and their corresponding trend were assessed for the twelve stations used in this study and the results are presented. The temporal variability was assessed using a time series analysis which involved plotting rainfall against the time using python tool, statistical measures were done using Instat tool while spatial variability of rainfall was analyzed and plotted using Surfer software that provided spatial maps, thus this method enabled us to know how rainfall varies geographically across the country.

Several statistical measures were performed in assessing the performance of CORDEX models in simulating the present climate Rwanda. The Climate Data Operator (CDO) was used in data manipulation while Grid Analysis and Display System (GrADS) tool was used in plotting the resulting maps. It worth noting that all the tables and figures are put in the addendum 1 and 2 respectively.

4.1 results from tests for data homogeneity

The methods that are normally employed to detect and correct inconsistence in the data set are single and double mass curves. The single mass curve was used in this study to tests for the homogeneity of the data. Single mass curve results **(Figure 3)** show the plots of annual cumulative rainfall against time; the mass curves were almost straight lines indicating that data are homogeneous and data is of good quality.

4.2. spatial-temporal analysis of rainfall

Spatial-temporal analysis of rainfall during rain seasons and annual time scale and their corresponding trend were assessed and the results are summarized in the next subsections.

4.2.1 Spatial rainfall distribution

To assess the spatial distribution of mean rainfall over Rwanda during MAM, OND and annual time scale in the period of 1981 to 2017, the seasonal and annual mean rainfall have been analyzed and the results are presented in **Table 3.** The spatial distribution of the mean rainfall during MAM, OND and annual time scale has been plotted using Surfer software and the results are presented in **Figure 4, 5 and 6** for MAM, OND and annual time scale respectively. In general, the rainfall increases from eastern to western parts of the country. The results indicated that rainfall amount ranges from 304mm to 473mm **(Figure 4)**, from 293 mm to 497 mm **(Figure 5)** and 842 mm to 1436 mm **(Figure 6)** during MAM, OND and annual time scale respectively.

The minimum is in the northeast regions (Nyagatare), eastern parts(Kayonza and Ngoma) increasing towards the central plateau (Kigali and Byimana) while the maximum is located in the highland region all along Congo Nil Crest extending to the Nyungwe natural Park, Virunga National park, southwestern parts (Rubona, Nyamagabe, Kamembe) and over northern parts (Gicumbi and Musanze). The rainfall distribution shows that much of rainfall are observed in the highland area compared to low land area which indicate that the topography plays an important role in the distribution of rainfall over Rwanda. The results of spatial rainfall distribution confirm the results obtained by[3].

4.2.2. Temporal rainfall variability

Temporal rainfall variability with their corresponding trend during the long rain season (MAM), short rain season (OND) and on annual time scale, was investigated using a graphical method and the results indicate a clear rainfall variability, where increasing and decreasing trend being non-uniform across all stations considered under this study. The significance of the trend was assessed using Mann Kendal non-parametric test and reported at 95% significance level while Sen's slope estimator was used to determine the magnitude of the trend. The Mann Kendal test results are summarized in the table4 below for March to May, October to December and annual time scale respectively.

4.2.2.1. Results of trend analysis

In this study the trend analysis during the long rain season (MAM), short rain season (OND) and on annual time scale was determined through a graphical plot of the rainfall data series and statistical methods.

4.2.2.2 Results from graphical method

The results of trends analysis from graphical method were classified into two categories namely increasing trends (positive) and decreasing trends (negative).The analysis of rainfall data for all stations showed that there are trends during MAM, OND and annual time scale. Temporal rainfall variability during the long rain season (MAM), short rain season (OND) and on annual time scale indicate a clear rainfall variability, where increasing and decreasing trend being non-uniform across all stations considered under this study.

The trend results from graphical method during March to May season (**Figure 7)** and annual time scale **(Figure 9)** indicate an increasing rainfall trend over Rubavu (north western) while Nyagatare (north eastern), Kayonza (central eastern), Ngoma (south eastern), Kigali (Kigali city) Byimana, Rubona and Nyamagabe (Southern), Kamembe (south western), Rubengera (central western) Musanze and Gicumbi (northern) stations show a decreasing rainfall trend respectively. Generally, these results reveal that the March to May season show a decreasing rainfall trend and the resulting trend may affect social economic sectors due to the fact that this season is the main rainfall season over Rwanda. The trend results obtained confirms the results of [11][100][101][102][103]. On longer timescales, total precipitation received during the long rains season has been reported to be in decline in recent decades[11][101][102]. This decline has been attributed to upward trend in SSTs in the south-central Indian Ocean[11] and west Pacific Ocean[102][103] which favor a local enhancement of precipitation with the resultant latent heating altering regional wind and moisture flux patterns, thereby reducing long rains precipitation in East Africa [101]. Other studies have shown that on multi-decadal and longer time scales, there is no strong signal in rainfall variability on longer time scales for East Africa, however, there is some evidence that the gradient of SSTs across the Indian Ocean plays an important role in influencing this variability[104].

The trend results from graphical method during October to December season **(Figure 8)** reveals a deceasing trend over Gicumbi (northern), Kamembe (south western), Ngoma (south eastern), Nyagatare(north eastern) and Nyamagabe(Southern) while Kayonza (central eastern), Kigali (Kigali city), Byimana, Rubona and Nyamagabe (southern), Rubengera (central western) and Rubavu (north western) stations show an increasing rainfall trend. The results obtained in this study confirms the results of [20][30] [105]. It was further indicated that over East African, the enhanced OND rainfall are predominantly driven by the local warm SST anomalies in the western equatorial Indian Ocean, while the eastern cold pole of the tropical IOD is of lesser importance[105]. Seasonally, the ENSO teleconnection influence is most strongly pronounced in the OND rain season [20][30].

4.2.2.3 Results from Statistical Analysis of Trends

Statistical methods were used to test the significance of the trend. The trend analysis using Mann Kendal non-parametric test and magnitude of the trend using Sen's slope estimator reported at 95% significance level were performed and the results obtained **(Table 4)** suggest that there were trends. However at 95% confidence level, there is sufficient statistical evidence to conclude that there a significant rainfall trend over Gicumbi (Northern) and Kamembe (south western) during MAM, OND and annual time scale and a significant rainfall trend over Nyamagabe and Rubona (southern) during MAM and annual time scale.

Furthermore, result from statistical method **(Table 4)** show a non-significant decreasing rainfall trend over Ngoma (south eastern) and Nyagatare (North eastern) during MAM, OND and annual time scale, Kayonza(central eastern), Kigali(Kigali city), Musanze (Northern), Rubengera (central western) and Byimana (southern) during MAM and annual time scale while a non-significant increasing trend was observed over Rubavu (north western) during MAM season, Byimana and Rubona (southern), Rubengera (central western), Musanze (Northern), Kigali (Kigali city) and Kayonza (central eastern) during OND season at 95% confidence level.

4.2.2.4 Results from Coefficient of variation and reliability

In this study an attempt has been made to examine variability and reliability of seasonal as well as annual rainfall records using method of the coefficient of variation and reliability. The coefficient of variation (CV) and the reliability (R) for long rain season (March –May), short rain season (October – December) and annual time scale have been determined using the Instat software and the obtained coefficient of variation results **(Table 5)** during the long rain season (MAM) ranges between 20-32%. The spatial distribution of coefficient of variation **(Figure 10)** indicates that the highest coefficient of variation was observed over the north eastern parts of the country (Nyagatare and Gatsibo) extending to the eastern part of the norther province (Gicumbi) and north western parts of the country (Rubavu) indicating low rainfall reliability over these regions. It is also important to indicate that the rest of the country exhibits low coefficient of variation indicating high rainfall reliability over these regions during March to May rain season.

Furthermore, an attempt has been made to examine variability and reliability during the OND rainy season and the results indicate that the coefficient of variation **(Table 5)** during the short rain season (OND) ranges between 18-37%. The spatial distribution of coefficient of variation **(Figure 11)** indicates that the highest coefficient of variation revealed that the highest coefficient of variation was observed over the north eastern parts of the country (Nyagatare and Gatsibo) and the central part of the southern province towards the central part of the western province indicating low rainfall reliability over these regions. The lowest coefficient of variation was observed over Kigali (Kigali city); Northern Province, south western extending from Nyamagabe to Kamembe and the area bordering lac Kivu and this may results from the impacts of highland, Virunga and Nyungwe national parks and the lac Kivu. The extent to which these features influence the rainfall distribution during short rain season is not well documented and there is need to further investigate their contribution to the OND rainfall distribution.

On annual time scale, examining the rainfall variability and reliability was quite important to understand it spatial distribution. On annual time scale, the coefficient of variation **(Table 5)** ranges between 14 and 31%. The highest rainfall variability **(Figure 12)** was observed over the north eastern parts (Nyagatare and Gatsibo) extending to the rest of the eastern province and the north eastern part of the Northern Province. This shows that there is low rainfall reliability over the eastern part of the country indicating that there is a challenge in predicting rainfall over the eastern region.

In addition, the comparison of annual and seasonal rainfall variability, results showed that there is higher seasonal variation than annual variation with March to May rainfall season being more reliable than October to December rainfall season, indicating that the high rainfall variability observed during OND season results into low rainfall reliability which may affects greatly the agricultural sector. Furthermore, the comparison of annual and seasonal rainfall variability shows that annual rainfall is higher and more reliable than seasonal rainfall.

4.3 Assessing the performance of CORDEX models to simulate the climate of Rwanda

To assess the models performance, which is the second specific objective of this study, statistical measures were used to assess the performance of CORDEX models to simulate the climate of Rwanda, statistical measures such as Pearson correlation coefficient(r) [91][92][93],[97], Mean absolute error (MAE) [91] and the index of agreement (d)[91] were performed to check the accuracy, bias, and reliability of the generated data compared to the observed rainfall from Meteo Rwanda data[91] for the six CORDEX models during MAM and OND rain seasons and the results are presented.

4.3.1 Correlation coefficient (r)

The correlation coefficient(r) was used to measure the level of association between the observed values and the model outputs. A correlation coefficient of 1.0 denotes positive linear relation while correlation coefficient of -1.0 denotes a negative linear relationship in the observed and model outputs values. A correlation coefficient equal to 0.0 represents no association between the two variables the observed values and the model outputs. The correlation coefficient between observed and CORDEX model outputs during long rain season (MAM) and short rain season (OND) were carried out to assess the relationship between CORDEX model outputs and observed rainfall for the twelve stations used under this study.

The correlation coefficient results **(Table 6)** indicated a week correlation between all CORDEX model and observation was observed during both long rain season (MAM) and short rain season (OND) respectively. For the six models used in this work, the IPSL and CCCma CORDEX models have revealed a relatively week positive correlation during MAM and OND rain seasons respectively. For the interest of the long rain and short rain seasonal prediction, we have adopted the IPSL and CCCma CORDEX models to be used in projecting the future long rain and short rain seasons respectively.

4.3.2 Mean absolute error (MAE)

The mean absolute error (MAE) is the arithmetic average of absolute differences between the observed and predicted values and ranges between zero and large positive values[91]. It has been indicated that MAE is a more natural measure of average error than RMSE and it is recommended that the evaluation and inter-comparisons of average model-performance error should be based on MAE.[94][95][96]. The mean absolute error results **(Table 7)**, indicate a bias between CORDEX models and observed rainfall during the long rain and short rain season respectively

4.3.3 Index of agreement (d)

The index of agreement (d) is the ratio of the mean square error and the potential error multiplied by number of observation and then subtracted from one [91]. The relative accuracy measure‘d’ accounts for the differences between means and variances of Predicted and observed and ranges between 0.0 and 1. Values close to 1 indicates better agreement between the predicted and observed [93][91]. During the long rain season **(Table 8)**, the IPSL model revealed a reasonable good index of agreement between model and observation while CCCma model present a reasonable good index of agreement **(Table 8)**, between model and observation during short rain season.

4.3.4 Rainfall Climatology difference

The difference between the CORDEX models and long rain observed rainfall data indicate how the model over (under) estimate the observed rainfall during MAM rain season for each grid cell. The result of the difference plot during MAM rain season **(Figure 13)** indicate a slight underestimation of long rainfall mean over northern, and a slight over estimation over the central and eastern part of the county. All models fail to capture the feature observed in the data over the area around Muhanga and Ngororero.

The difference between the CORDEX models and observed rainfall data during the short rain season indicate how the model over (under) estimate the observed rainfall data for each grid cell during OND rain season. The difference plot results (**Figure 14)** reveal a slight over estimation of short rain seasonal mean over northern, and a slight under estimation over the central and eastern part the of the county. A high under estimation was revealed over the southwestern part of the country.

4.4 Rainfall projection

In this work, the projected rainfall during MAM rain season was conducted based on the IPSL model while the CCCma model was used to project the OND rainfall respectively. In this work, the RCP 4.5 and RCP 8.5 were used. To account for bias in the model, a simple linear regression model (**Table 9)** was develop between the observed data and the historical model data for both models during MAM and OND rain seasons to determine the linear regression coefficient which have been used to re produce the projected data under both RCP 4.5 and RCP 8.5 and the resulted projection has been generated using the following coefficients.

4.4.1 Rainfall projection during March to May rain season

The projected long rain season (MAM) rainfall was carried out using the IPSL model output corrected using the simple linear regression coefficient. The representative concentration pathways (RCP 4.5 and 8.5) were selected in this study.

The temporal variability of the projected rainfall during 2020-2049 was carried out and the results indicate an increasing trend in projected long rain seasonal rainfall **(Figure 15)** will be experienced over Gicumbi, Musanze Nyamagabe, Rubengera and Byimana respectively while a decreasing trend will be experienced over Kamembe, Rubavu, Kigali, Nyagatare, Kayonza and Ngoma under RCP 4.5 respectively.

During long rain season, a decreasing trend **(Figure 16)** will be experienced over Kamembe, Rubona, Rubengera, Musanze Kigali and Gicumbi respectively while an increasing trend in projected long rain seasonal rainfall will be experienced over Rubavu, Nyamagabe, Kayonza, Ngoma, Nyagatare and Byimana under RCP8.5 respectively .

4.4.2 Rainfall projection during October to December rain season

The short rain season (OND) projection using the CCCma model output corrected using the simple linear regression coefficient was assessed. The representative concentration pathways (RCP 4.5 and 8.5) were selected in this study.

The Projected short rain seasonal rainfall **(Figure 17)** during 2020 to 2049 will experience An increased rainfall trend over Gicumbi, Musanze Nyamagabe, Rubengera and Byimana respectively while a decreasing trend will be experienced over Kamembe, Rubavu, Kigali, Nyagatare, Kayonza and Ngoma under RCP 4.5 respectively.

During long rain season, a decreasing trend **(Figure 18)** will be experienced over Kamembe, Rubona, Rubengera, Musanze Kigali and Gicumbi respectively while an increasing trend in projected long rain seasonal rainfall will be experienced over Rubavu, Nyamagabe, Kayonza, Ngoma, Nyagatare and Byimana under RCP8.5 respectively.

4.4.3 Projected rainfall change during MAM seasonal rainfall

The projected rainfall change which consist of the difference between the projected mean rainfall during 2020 -2049 and the observed mean rainfall during 1981-2010 base line was analyzed and the obtained results are discussed in the next sub sections.

The projected rainfall change results in millimeters and percentage (**Table 10)** during MAM rain season and also represented graphically **(Figures 19)** indicate a projected decrease in rainfall of 5% and 5 to 6% over Nyamagabe and Rubavu under both RCP 4.5 and RCP 8.5 respectively while other stations will exhibit an increase in rainfall of 2 to 6 % and 1 to 5% under both RCP8.5 and RCP4.5 respectively during MAM rain season.

4.4.4 Projected rainfall change during OND seasonal rainfall

The projected rainfall change which consist of the difference between the projected mean rainfall during 2020 -2049 and the observed mean rainfall during 1981-2010 baselines during the short rain season using the CCCma model under RCP4.5 and RCP 8.5 was analyzed and the obtained results are discussed in the next sub sections.

The projected rainfall change results in millimeters and percentage (**Table 11)** during MAM rain season and also represented graphically **(Figures 20)** revealed a projected decrease rainfall of 3% over Musanze, 5% over Nyamagabe, 1% over Rubona and Byimana, 3 to 4% over Kigali and 4% Rubengera under both RCP8.5 and RCP4.5 respectively. Ngoma revealed a decreasing rainfall of 1% under RCP8.5 and an increasing of rainfall of 1% under RCP4.5 while Kayonza will exhibit an increasing rainfall of 5% under RCP8.5 and a decreasing rainfall of 2% under RCP4.5. A projected increase in rainfall ranging from 1 to 5% will be experienced over Nyagatare, Gicumbi and Kamembe under both RCP 8.5 and RCP 4.5 respectively. It is important to note that the projected change over Kayonza and Ngoma are not consistent under both RCPs which indicate uncertainty over the East-Rwandan hot and dry lowland climatological zone.

It should be clear that even though we have used model simulations for individual runs which produce an individual time series of 2020-2049, the more important information to glean is the statistical information. Individual GCM simulations should not be taken literally as probable 30 year forecasts of what will happen.

CHAPTER FIVE

5.0 CONCLUSION AND RECOMMANDATIONS

The main objective of this study was to determine the rainfall variability and projected change in Rwanda. The study utilized graphical and statistical methods to assess the trend in rainfall variability. To assess the skill of the models in simulating the climate of Rwanda, correlation, absolute mean error, index of agreement and rainfall climatology difference plots analysis were used. The spatial-temporal variability of rainfall during rain seasons and annual time scale, the assessment the performance of CORDEX models to simulate the climate and the projected rainfall change under RCP4.5 and RCP8.5 over Rwanda have been carried out.

The distribution of mean rainfall during long and short rain season as well as the annual time scale show that high rainfall are concentrated over the high land and southwestern parts which reduces toward the central parts while the low rainfall amount are observed in the Eastern part of the country. The trends result from graphical method indicates clear rainfall variability, where increasing and decreasing trend being non-uniform across all stations considered under this study. The trend significance was carried out using statistical methods at 95% significance level, show that there is a significant increasing rainfall trend over Northern part of the Northern Province and southern province while a non-significant decreasing rainfall trend was observed over eastern, Kigali city, Northern and central western during MAM, and annual time scale. Furthermore, results indicate that the north eastern part of the country exhibits a more variable rainfall.

Statistical and graphical measures were used to assess the performance of CORDEX models in simulating the climate of Rwanda. The IPSL and CCCma models have revealed a better performance in simulating the climate of Rwanda during MAM and OND rain season respectively compared to the other models used in study. A simple linear regression model was developed to reproduce the projected rainfall under both RCP 4.5 and RCP8.5 for the IPSL and CCCma models which have been used o projected MAM and OND seasonal rainfall.

The projected rainfall change results indicated that MAM rainfall will exhibit a decreasing rainfall while OND will experience an increasing rainfall over Rwanda under both RCP4.5 and

RCP8.5 although models do not agree on the same increasing (decreasing) magnitude. All the six selected CORDEX models were not able to resolve the geographical features of the country where over (under) estimation of rainfall was observed during both long and short rain seasons as well as on annual time scale.

The results indicate that the north eastern part of the country exhibits a more variable rainfall during both long and short rain seasons as well as on annual time scale. It is recommended that further study should be carried out to investigate the intra seasonal rainfall variability over the region. The low rainfall variability was mainly observed over the highland and area bordering lac Kivu, study investigating the effect of lac Kivu in influencing the rainfall pattern of Rwanda is recommended.

It is highly recommended that planning and decision making in agricultural and water sector should reflect the rainfall variability and pattern both on seasonal and intra seasonal time scale in order to cope with the various effects associated with the rainfall variability. It is also recommended to conduct a detailed study on the intra- seasonal rainfall variability and predictability over Rwanda for better utilization of weather and climate services and products in social economic sectors of the country.

Six selected CORDEX models were considered under this study, it is recommended that further research should be conducted assessing the performance of all CORDEX models and bias correction measure should be undertaken and more stations should be used to represent the coverage of the country.

Due to the complex nature of Rwanda, it is strongly recommended that more studies could be done by using regional climate models designed over the Rwandan domain to capture the influence of the topography.

ADDENDUM 1: LIST OF TABLES

Table 1: CORDEX models used in this study

	INSTITUTE	GCM NAME
1	CCCma (Canada)	CanESM2
2	MOHC (UK)	HadGEM2-ES
3	ICHEC (Europe)	EC-EARTH
4	MIROC (Japan)	MIROC5
5	MPI-M (Germany)	MPI-ESM-LR
6	IPSL (France)	IPSL-CM5A-LR

Table 2: Representative Concentration Pathways (RCPs)

RCP	**Forcing**
RCP4.5	Stabilization scenario whereby the total radiative forcing is stabilized shortly after 2100. This will be achieved by adopting several technologies and strategies to cut GHG emissions [106]. More details can be found in [107] [108][109]
RCP8.5	This is 'business-as-usual' scenario. It is characterized by rising radiative forcing pathway leading to 8.5W m^{-2} by 2100, with forcing increasing further thereafter up to 12 W m^{-2} by 2250, when concentrations stabilize[110]. More details can be found in [107] [108][109]

Table 3: Mean rainfall (mm) for March - May (MAM); October - December (OND) and Annual Rainfall respectively from 1981 to 2017.

Stations	MAM	OND	Annual
	Mean (mm)	Mean (mm)	Mean (mm)
Gicumbi	462	373	1158
Kamembe	475	367	1436
Kayonza	336	293	863
Kigali	348	314	934
Musanze	440	419	1205
Ngoma	346	330	927
Nyagatare	304	318	842
Nyamagabe	416	349	1061
Rubavu	380	381	1138
Rubengera	408	350	1065
Rubona	413	351	1046
Byimana	425	349	1089

Table 4: Rainfall trend and magnitude (mm/year) during March to May, October to December and annual time scale from 1981 to 2017.

Time series	First year	Last Year	n	MAM			OND			Annual		
				Test Z	Sig	Q	Test Z	Sig	Q	Test Z	Sig	Q
Gicumbi	1981	2017	37	-3.2	*	-11.8	-2.5	*	-4.1	-3.2	*	-11.8
Kamembe	1981	2017	37	-3.1	*	-11.5	-3.8	*	-4.9	-3.1	*	-11.5
Kayonza	1981	2017	37	-0.7		-1.4	0.3		0.3	-0.7		-1.4
Kigali	1981	2017	37	-0.5		-0.8	0.3		0.3	-0.5		-0.8
Musanze	1981	2017	37	-1.0		-2.9	0.6		0.9	-1.0		-2.9
Ngoma	1981	2017	37	-1.8	+	-4.7	-0.6		-1.0	-1.8	+	-4.7
Nyagatare	1981	2017	37	0.9		2.8	1.0		1.8	0.9		2.8
Nyamagabe	1981	2017	37	-3.0	*	-8.9	-0.3		-0.2	-3.0	*	-8.9
Rubavu	1981	2017	37	0.0		-0.1	1.5		1.6	0.0		-0.1
Rubengera	1981	2017	37	-0.8		-2.0	0.5		0.6	-0.8		-2.0
Rubona	1981	2017	37	-1.9	*	-4.9	0.7		0.7	-1.9	*	-4.9
Byimana	1981	2017	37	-1.3		-3.2	0.3		0.3	-1.3		-3.2

Where Sig (*, + and empty space) are significance level at α equal to 5%, 10% and greater than 10% respectively), Q is the Sen's slope (in mm/year), Test Z is the Mann Kendal trend, n is the number of observation (37years).

Table 5: Rainfall coefficient of variation (CV in %) and rainfall reliability (R in %) for March - May (MAM); October - December (OND) and the annual timescale respectively from 1981 to 2017.

Stations	MAM		OND		Annual	
	CV (%)	R (%)	CV (%)	R (%)	CV (%)	R (%)
Gicumbi	25	75	27	73	21	79
Kamembe	20	80	18	82	17	83
Kayonza	20	80	21	79	15	85
Kigali	21	79	22	78	16	84
Musanze	20	80	18	82	16	84
Ngoma	23	77	26	74	23	77
Nyagatare	32	68	37	63	31	69
Nyamagabe	24	76	22	78	16	84
Rubavu	25	75	19	81	16	84
Rubengera	24	76	23	77	14	86
Rubona	23	77	31	69	17	83
Byimana	22	78	30	70	16	84

Table 6: Correlation coefficient (r) between observed and model data during MAM and OND rain seasons from 1981 to 2005

Correlation coefficient (r)												
models	CCCMA		ICHEC		IPSL		MIROC		MOHC		MPI	
SEASONS	MAM	OND	MAM	OND	MAM	OND	MAM	OND	MAM	OND	MAM	OND
Gicumbi	-0.14	0.17	-0.15	-0.04	0.36	-0.16	-0.37	-0.26	-0.08	-0.2	0.13	0
Kamembe	-0.1	0.24	-0.23	-0.25	0.19	-0.04	-0.62	-0.08	-0.08	-0.2	0.01	-0.05
Kayonza	0.12	0.53	0	-0.26	0.1	-0.04	-0.06	0.08	-0.39	0.2	0.27	-0.2
Kigali	0.03	0.31	-0.28	-0.27	0.25	0.12	-0.12	-0.25	0.21	-0.1	0.2	0.14
Musanze	-0.17	0.16	0	-0.3	0.5	0.14	-0.11	-0.39	-0.45	-0.3	0.1	-0.03
Ngoma	0.01	0.11	-0.11	-0.05	-0.29	-0.45	-0.24	0.28	-0.07	0.3	0.05	-0.01
Nyagatare	0.04	0.36	-0.38	0.01	0.4	0.04	-0.37	-0.36	0.13	-0.3	-0.15	0.14
Nyamagabe	0.12	0.4	0.04	0.03	0.29	0.11	0.18	-0.27	-0.1	0.1	0.13	-0.04
Rubavu	0.01	0.11	-0.27	-0.25	0.43	0.18	-0.4	-0.26	-0.02	-0.2	-0.04	0.13
Rubengera	-0.13	0.27	-0.1	-0.08	-0.2	-0.25	0.19	0.12	-0.04	0.5	0.05	-0.26
Rubona	-0.06	0.19	-0.25	-0.11	0.23	0.02	-0.36	-0.35	-0.32	0	0.1	0.1
Byimana	-0.06	-0.05	-0.39	-0.24	0.26	0	-0.31	-0.1	-0.15	-0.2	-0.05	0.09

Table 7: Mean absolute error (MAE) in mm between observed and model during MAM and OND rain seasons from 1981 to 2005

Mean absolute error(MAE)												
models	CCCMA		ICHEC		IPSL		MIROC		MOHC		MPI	
SEASONS	MAM	OND	MAM	OND	MAM	OND	MAM	OND	MAM	OND	MAM	OND
Gicumbi	185.4	114.5	119.7	79.9	208.0	114.0	132.3	26.1	308.1	13.8	90.4	62.9
Kamembe	280.2	228.3	303.2	226.1	309.0	328.7	306.1	363.3	393.5	347.1	258.5	289.7
Kayonza	23.6	221.3	42.1	186.6	46.2	7.2	29.6	132.9	146.3	120.6	71.4	169.7
Kigali	39.7	273.3	140.8	243.9	36.4	20.8	103.7	190.6	101.3	144.0	160.9	189.3
Musanze	180.8	380.9	245.6	364.8	174.7	12.6	242.0	222.2	99.6	106.1	313.2	241.9
Ngoma	188.2	16.3	161.1	33.2	134.7	26.8	174.8	105.0	270.4	92.9	133.9	58.2
Nyagatare	152.5	8.7	116.8	8.2	156.4	111.6	130.5	80.0	226.1	67.9	89.6	33.1
Nyamagabe	219.8	524.8	199.5	554.1	117.5	219.3	195.9	314.3	103.2	295.3	309.8	385.8
Rubavu	130.5	41.6	68.4	31.1	26.1	68.7	14.1	130.1	182.1	5.2	14.9	14.7
Rubengera	32.2	268.4	57.7	286.6	5.2	35.8	49.8	135.3	177.7	104.6	132.4	182.4
Rubona	221.3	28.3	194.3	17.4	165.7	33.7	200.4	93.9	304.8	80.2	162.0	48.7
Byimana	212.2	23.1	185.2	12.3	156.6	28.6	228.4	112.2	295.7	75.0	152.9	43.6

Table 8: Index of agreement (d) between observed and model data during MAM and OND rain seasons from 1981 to 2005

Index of agreement(d)												
Models	CCCMA		ICHEC		IPSL		MIROC		MOHC		MPI	
SEASONS	MAM	OND	MAM	OND	MAM	OND	MAM	OND	MAM	OND	MAM	OND
Gicumbi	0.92	0.97	0.97	0.97	0.92	0.85	0.95	0.90	0.78	0.95	0.98	0.95
Kamembe	0.82	0.92	0.78	0.91	0.77	0.47	0.77	0.43	0.53	0.38	0.86	0.63
Kayonza	0.97	0.91	0.98	0.92	0.98	0.94	0.98	0.67	0.91	0.88	0.98	0.85
Kigali	0.97	0.89	0.96	0.90	0.99	0.94	0.96	0.34	0.94	0.88	0.95	0.84
Musanze	0.95	0.89	0.94	0.90	0.95	0.94	0.93	0.66	0.97	0.96	0.92	0.88
Ngoma	0.87	0.99	0.91	0.98	0.94	0.96	0.88	0.79	0.66	0.84	0.94	0.93
Nyagatare	0.89	0.99	0.94	0.98	0.8	0.71	0.92	0.80	0.70	0.88	0.96	0.92
Nyamagabe	0.93	0.79	0.94	0.66	0.97	0.86	0.92	0.07	0.95	0.80	0.91	0.75
Rubavu	0.93	0.99	0.97	0.97	0.97	0.90	0.97	0.83	0.87	0.96	0.98	0.90
Rubengera	0.97	0.90	0.97	0.89	0.98	0.94	0.96	0.77	0.89	0.93	0.97	0.88
Rubona	0.86	0.98	0.89	0.98	0.93	0.96	0.88	0.87	0.68	0.90	0.93	0.94
Byimana	0.87	0.98	0.90	0.98	0.94	0.94	0.83	0.78	0.69	0.90	0.94	0.94

Table 9: Linear regression coefficient between observed and model historical data from 1981 to 2005

Linear regression coefficients during MAM and OND rain seasons				
seasons	MAM		OND	
stations	a	b	a	b
Kayonza	0.2553	263.38	0.1723	195.72
Nyagatare	0.5181	230.36	0.55	131.07
Gicumbi	0.3111	408.92	0.252	262.34
Kamembe	0.1716	461.08	0.5302	366.48
Musanze	0.1501	553.84	0.042	384.19
Ngoma	0.52	248.02	0.4276	194.08
Nyamagabe	0.2723	288.66	0.0345	315.77
Rubavu	-0.1903	434.12	0.435	230.54
Rubona	0.4227	320.38	-0.0442	353.04
Byimana	0.5808	268.89	0.1644	283.01
Kigali	0.48188	191.49	0.1086	241.3
Rubengera	0.1897	344.55	0.0925	284.15

Table 10: Projected MAM rainfall change using RCP4.5 and RCP 8.5 from IPSL model from 2020 to 2049

Stations	RCP85(mm)	RCP45(mm)
Kayonza	17	12
Nyagatare	17	14
Gicumbi	17	16
Kamembe	14	15
Musanze	19	17
Ngoma	17	18
Nyamagabe	-21	-23
Rubavu	-25	-20
Rubona	15	15
Byimana	20	21
Kigali	9	3
Rubengera	6	6

Projected MAM rainfall change (mm) using RCP4.5 and RCP 8.5 from IPSL model for the twelve stations used under the study where positive (negative) value indicate an increase (decrease)

Table 11: Projected OND rainfall change using RCP4.5 and RCP 8.5 from CCCma model from 2020 to 2049

Stations	RCP85(mm)	RCP45(mm)
Kayonza	14	-5
Nyagatare	12	17
Gicumbi	5	2
Kamembe	19	13
Musanze	-14	-14
Ngoma	-2	4
Nyamagabe	-18	-19
Rubavu	8	5
Rubona	-3	-2
Byimana	-2	-4
Kigali	-9	-12
Rubengera	-13	-14

Projected OND rainfall change (mm) using RCP4.5 and RCP 8.5 from CCCma model for the twelve stations used under the study where positive (negative) value indicate an increase (decrease)

ADDENDUM 2: LIST OF FIGURES

Figure 1*: Rwanda administrative map.*

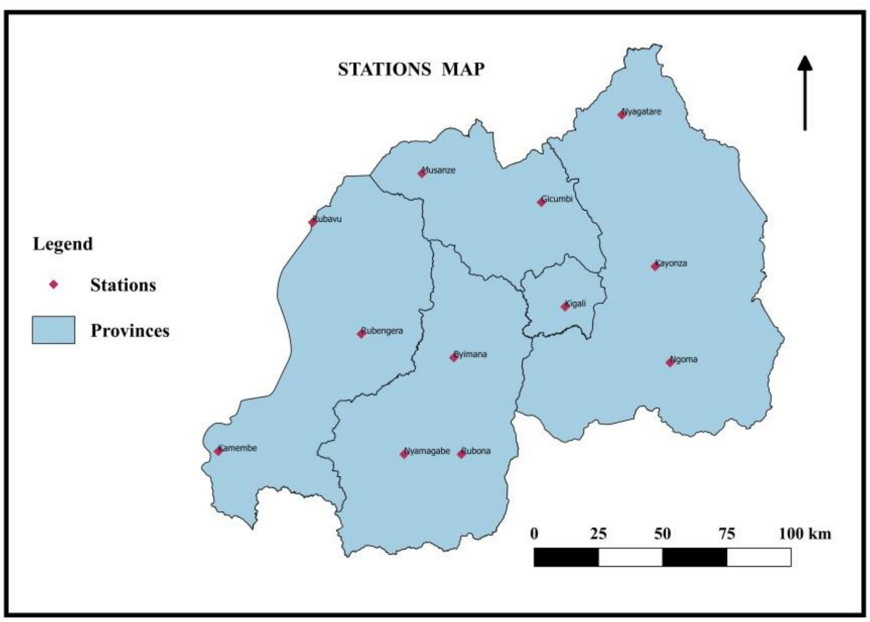

Figure 2 : *Location of the twelve rainfall stations used under this study*

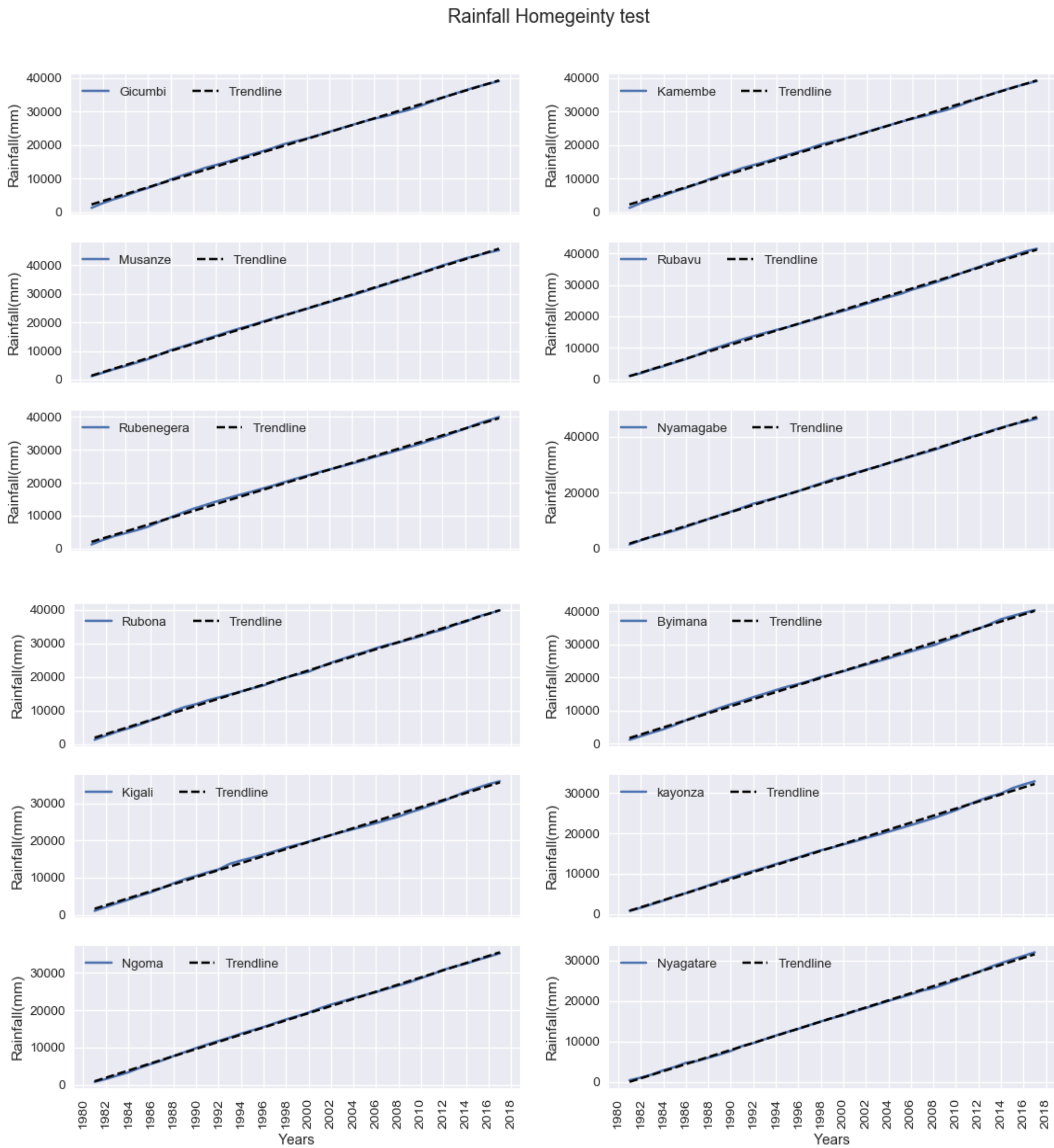

Figure 3*: single mass curve for the twelve stations from 1981 to 2017 (blue line is the cumulative annual rainfall, black line indicates the trend. because we are showing cumulative rainfall over many years, the "trend" doesn't necessarily indicate increasing rainfall, in fact it indicate that data are of good quality to be used in the study).*

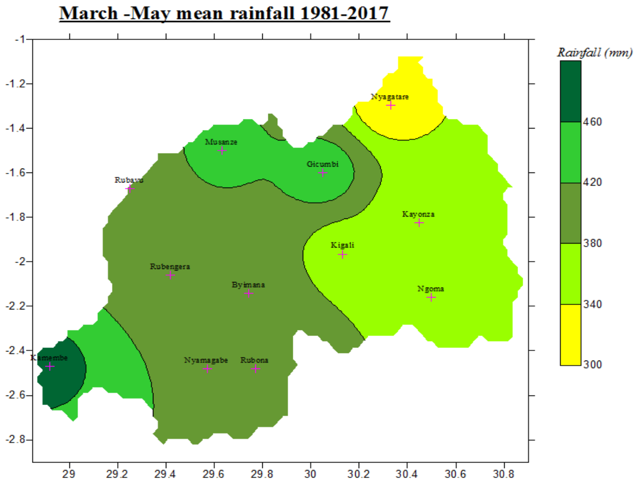

Figure 4: *Spatial mean rainfall distribution during March – May (MAM) rain season from 1981 to 2017.*

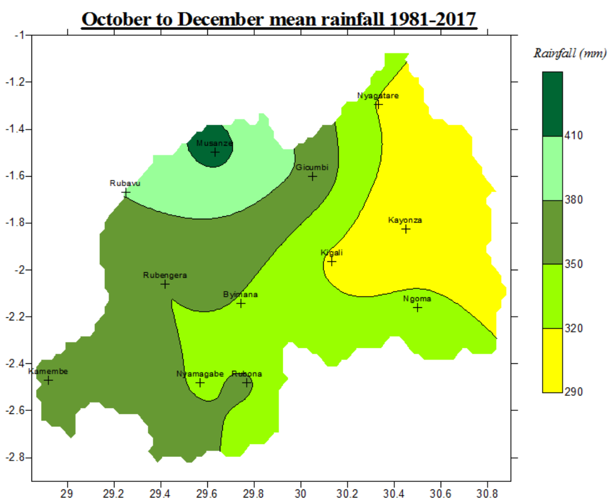

Figure 5*: Spatial mean rainfall distribution during October – December (OND) rain season from 1981 to 2017.*

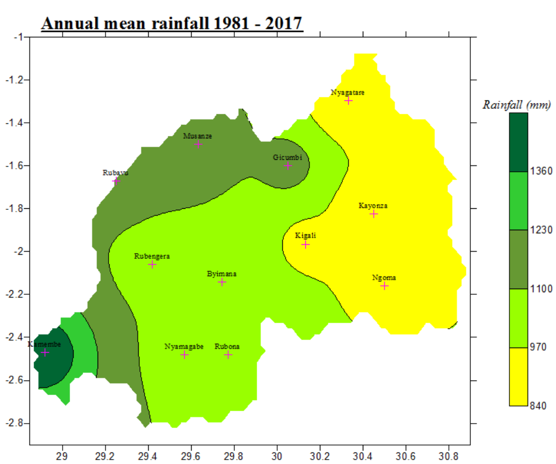

Figure 6: *Spatial annual mean rainfall distribution over Rwanda from 1981 to 2017.*

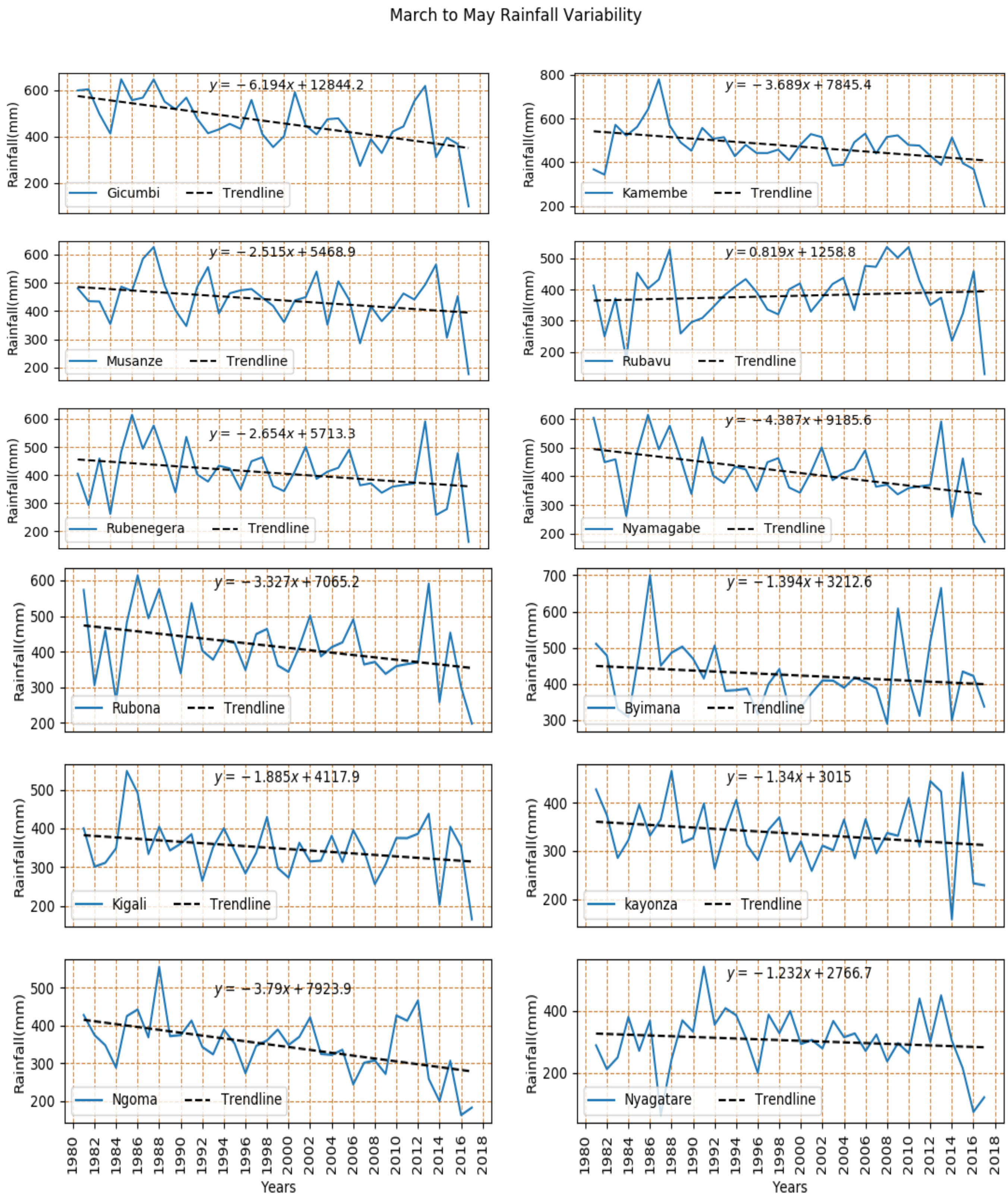

Figure 7*: Rainfall variability (mm) during March – May (MAM) rain season for the twelve stations from 1981 to 2017.*

.

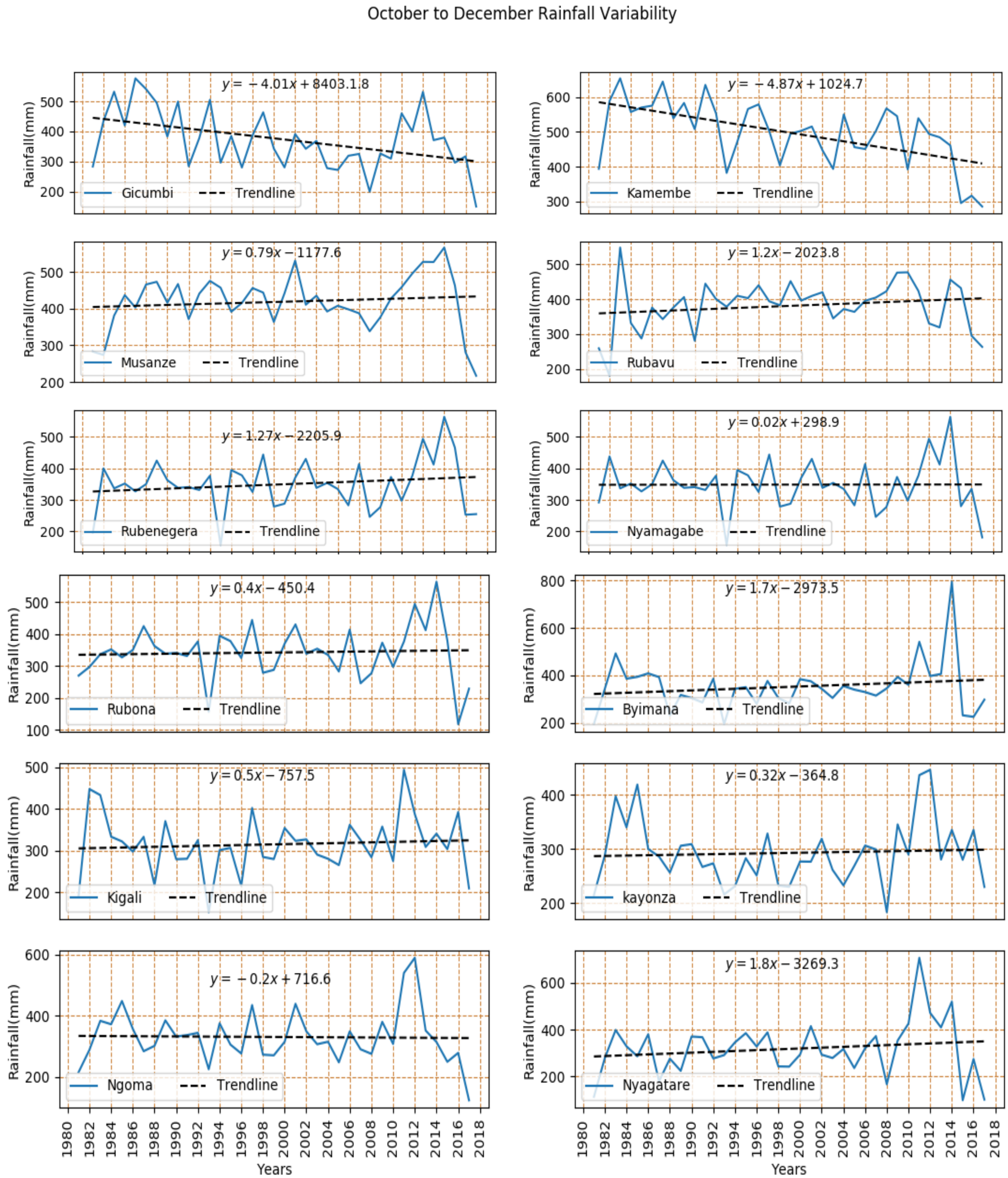

Figure 8: *Rainfall variability (mm) during October – December (OND) rain season for the twelve stations from 1981 to 2017.*

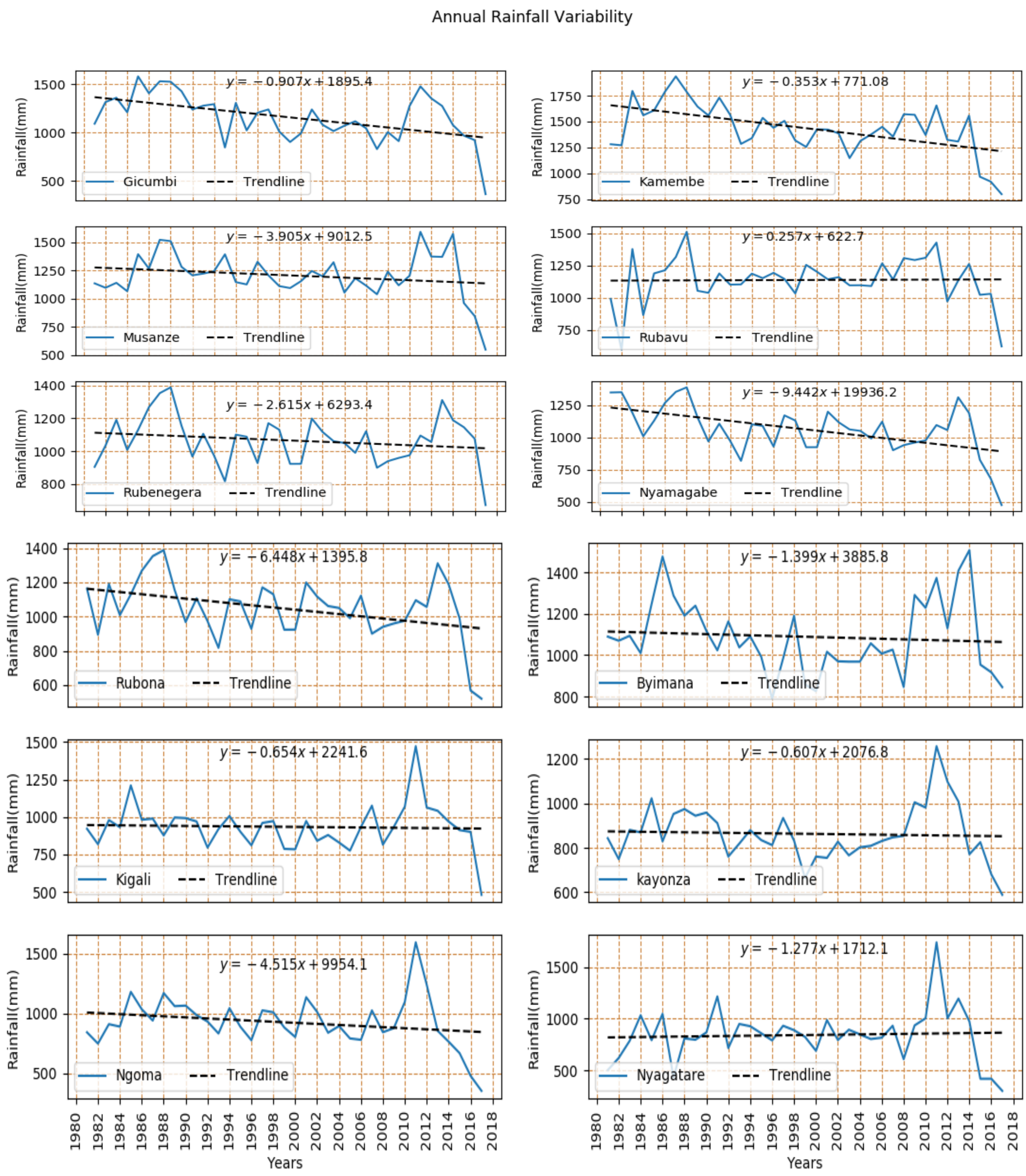

Figure 9: *Annual rainfall variability (mm) for the twelve stations from 1981 to 2017.*

.

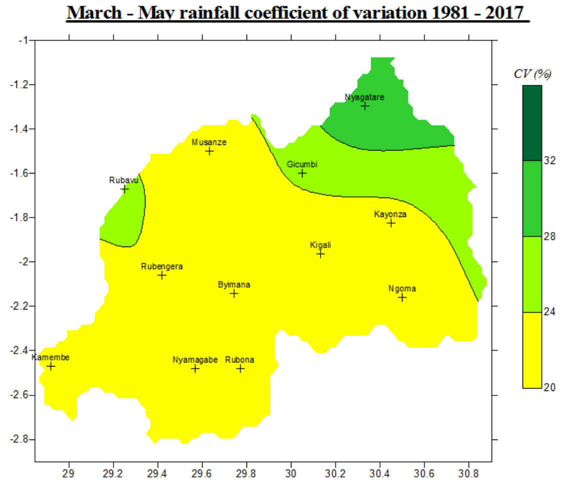

Figure 10: *Spatial coefficient of variation (CV) March to May (MAM) rain season from 1981 to 2017.*

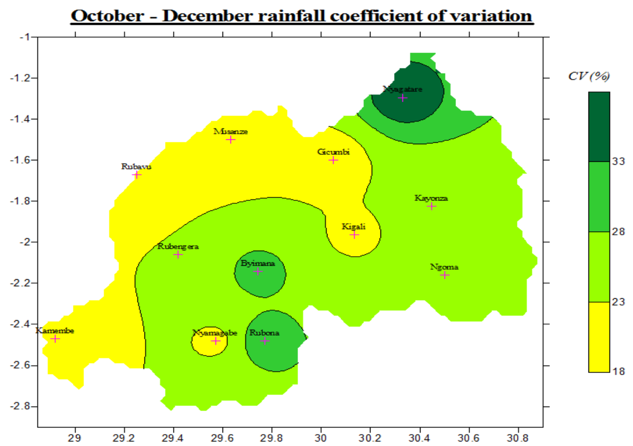

Figure 11: *Spatial coefficient of variation (CV) during October to December (OND) rain season from 1981 to 2017.*

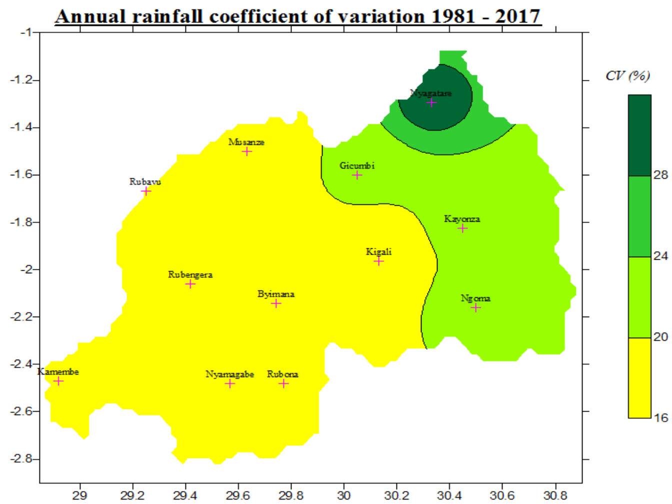

Figure 12: *Spatial annual coefficient of variation (CV) from 1981 to 2017.*

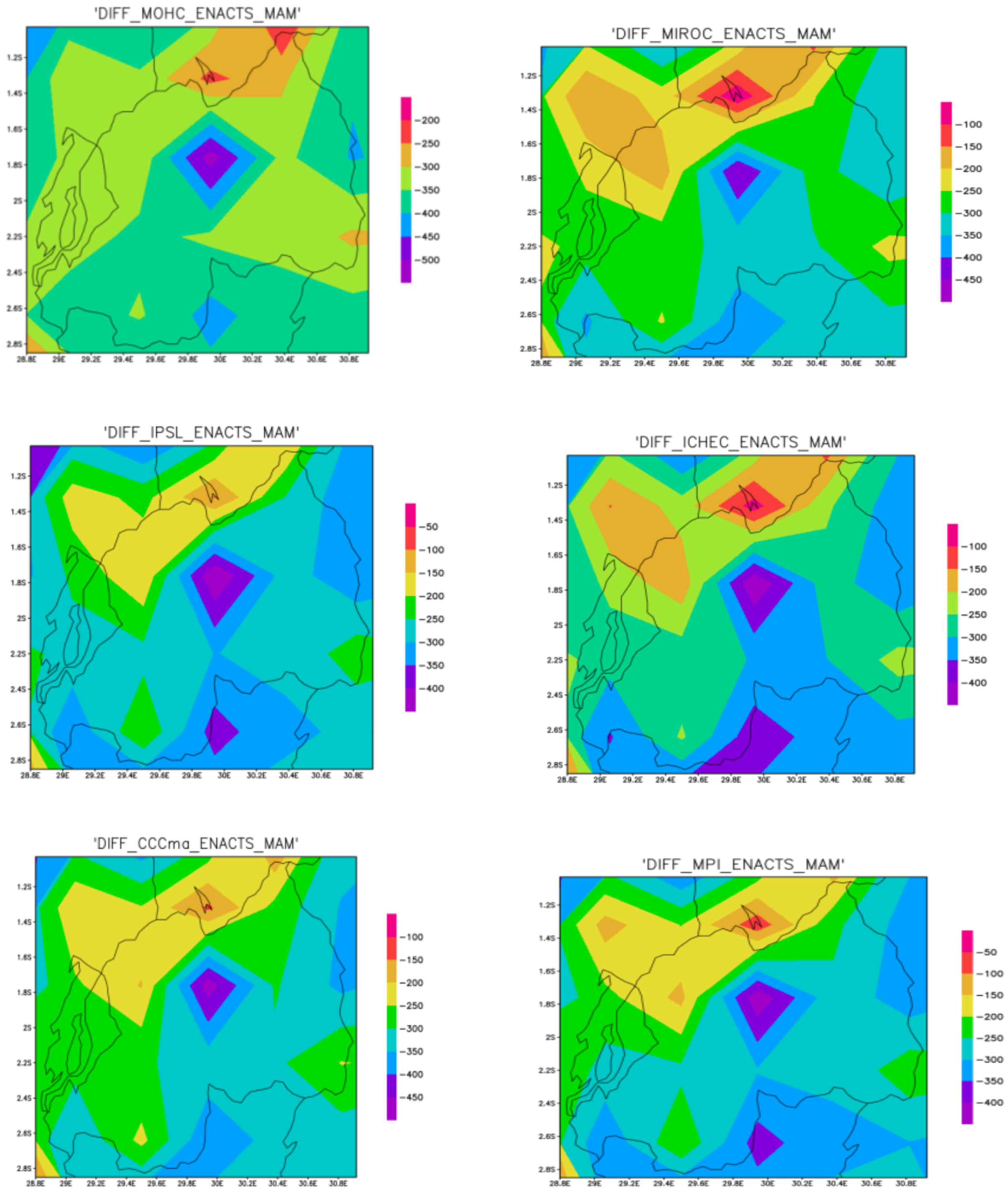

Figure 13: *Spatial rainfall difference distribution between models and the observed rainfall data during March – May (MAM) rain season from 1981 to 2005*

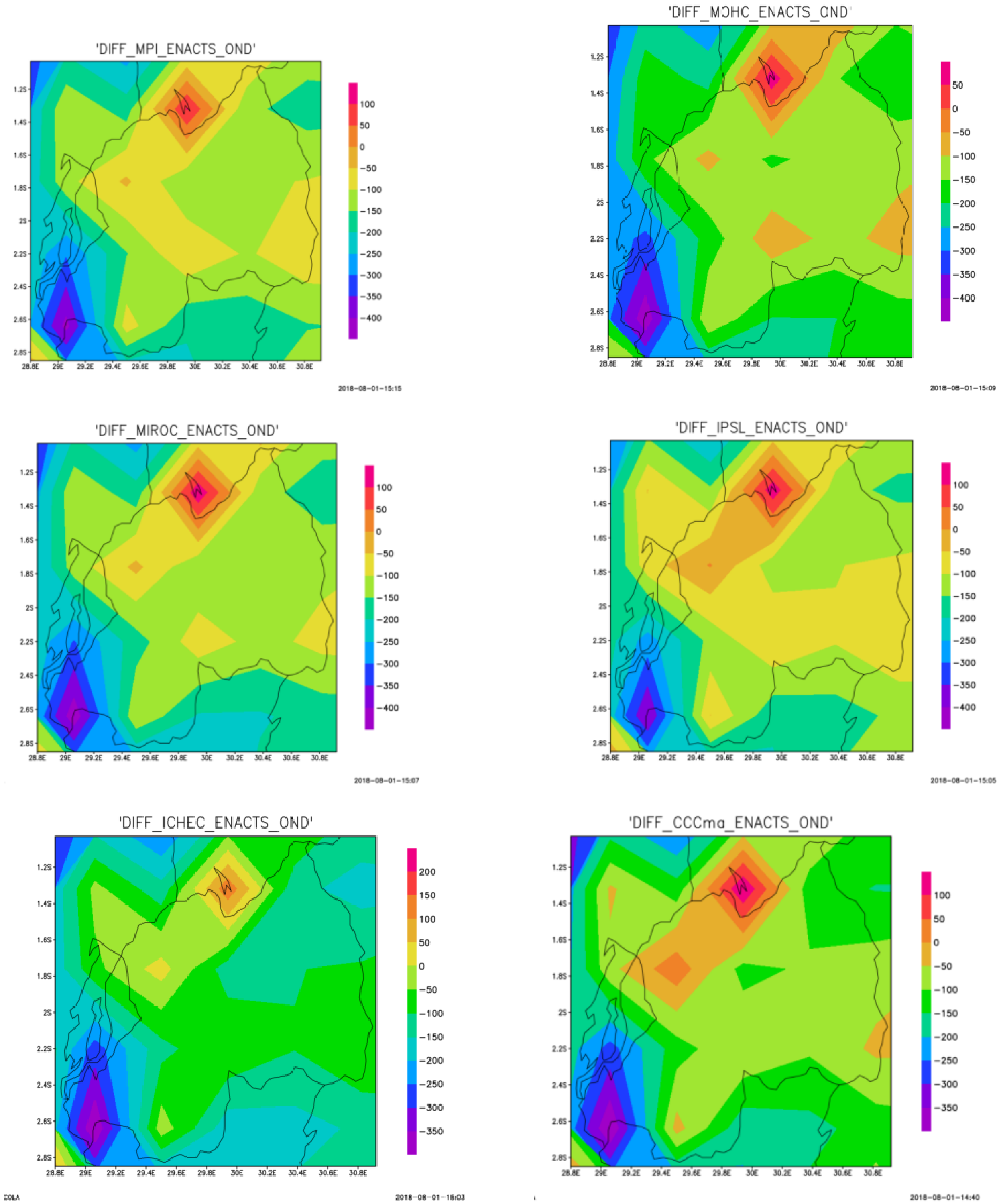

Figure 14: Spatial *rainfall difference distribution between the models observed rainfall during October –December (OND) rain season1981 to 2005*

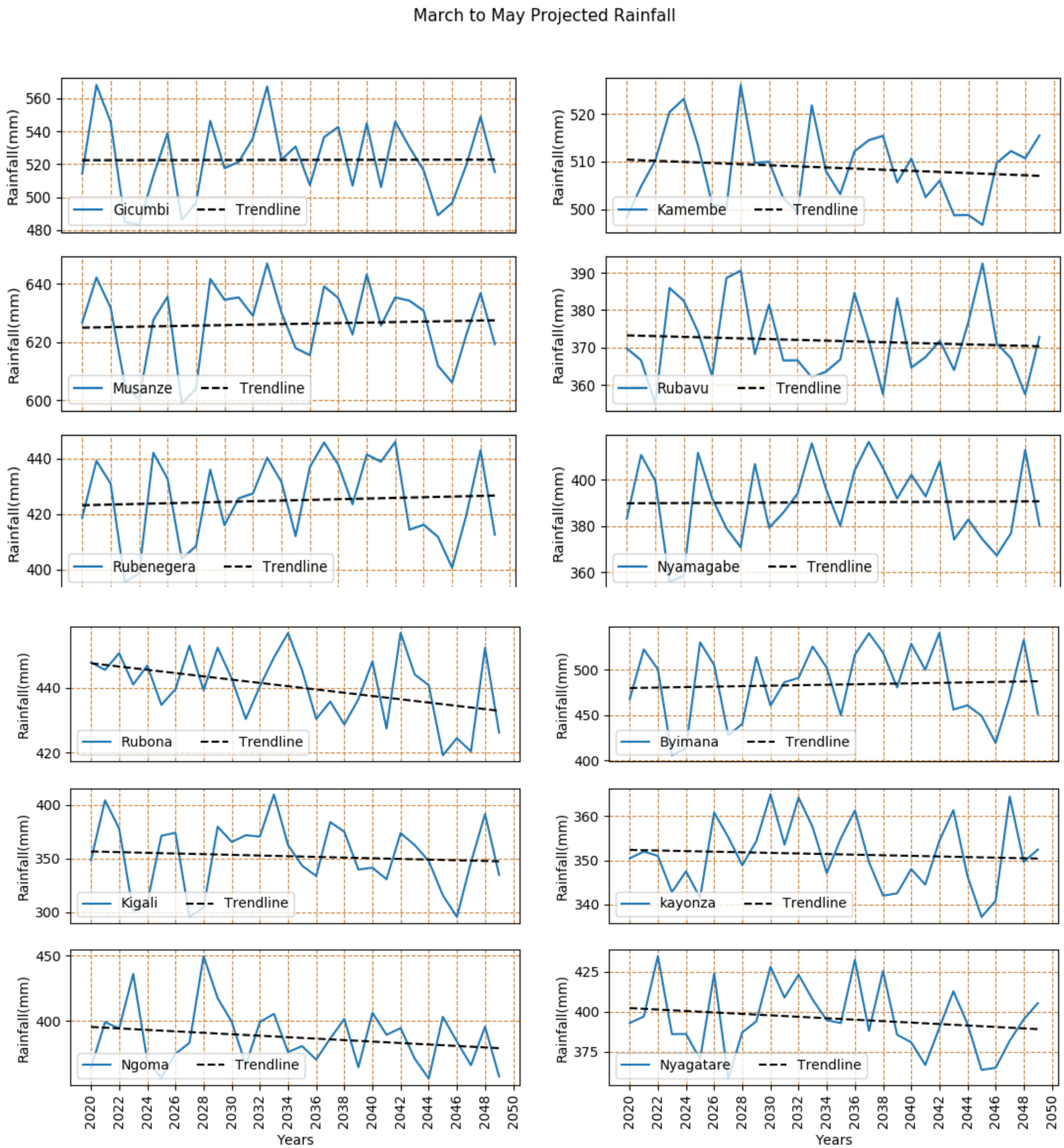

Figure 15: *Projected rainfall (2020-2049) using RCP4.5 from IPSL model during March to May rain season*

Figure 16: *Projected rainfall (2020-2049) under RCP8.5 from IPSL model during March to May rain season.*

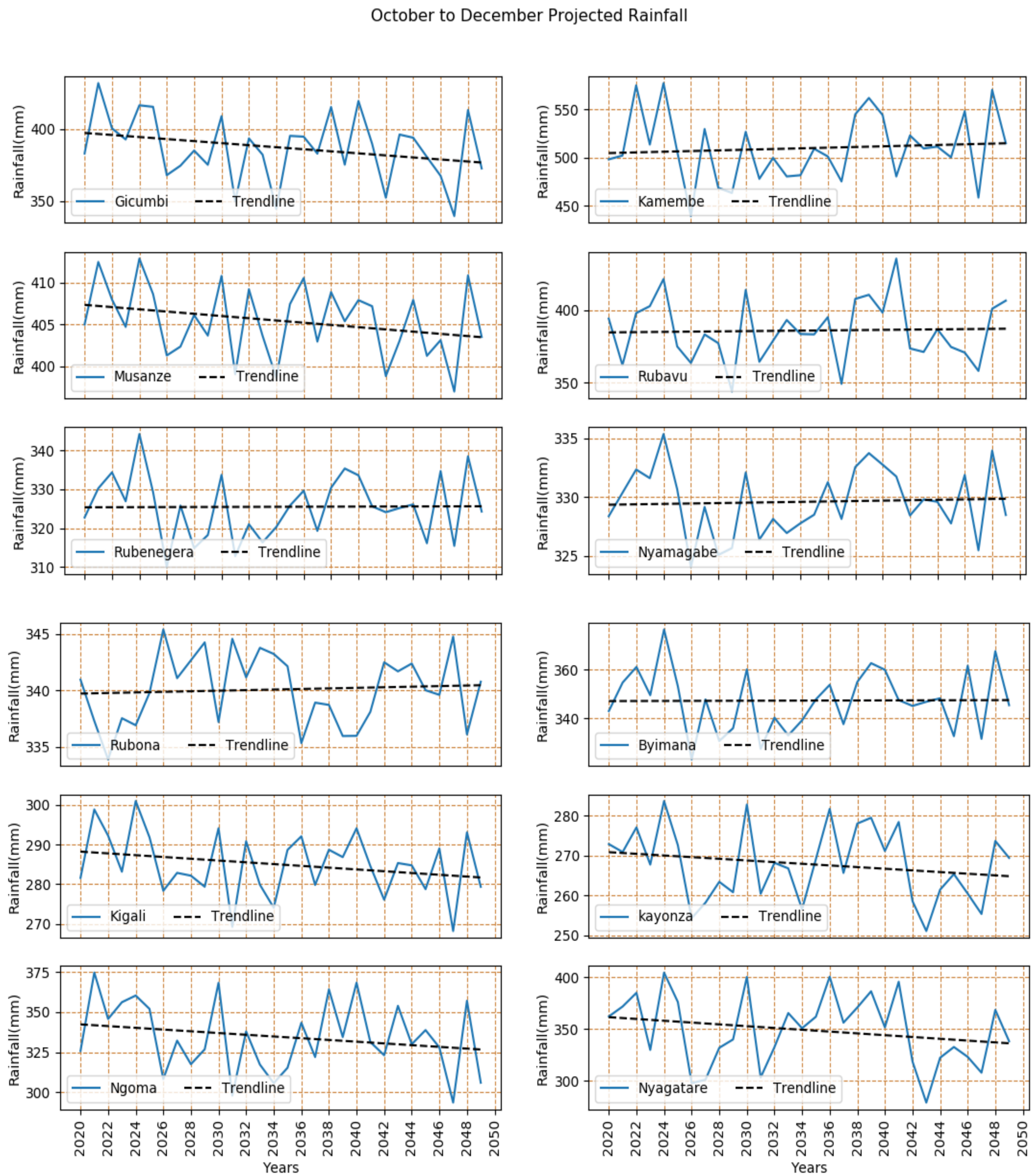

Figure 17: *Projected rainfall (2020-2049) using RCP4.5 from CCCma model during OND rain season.*

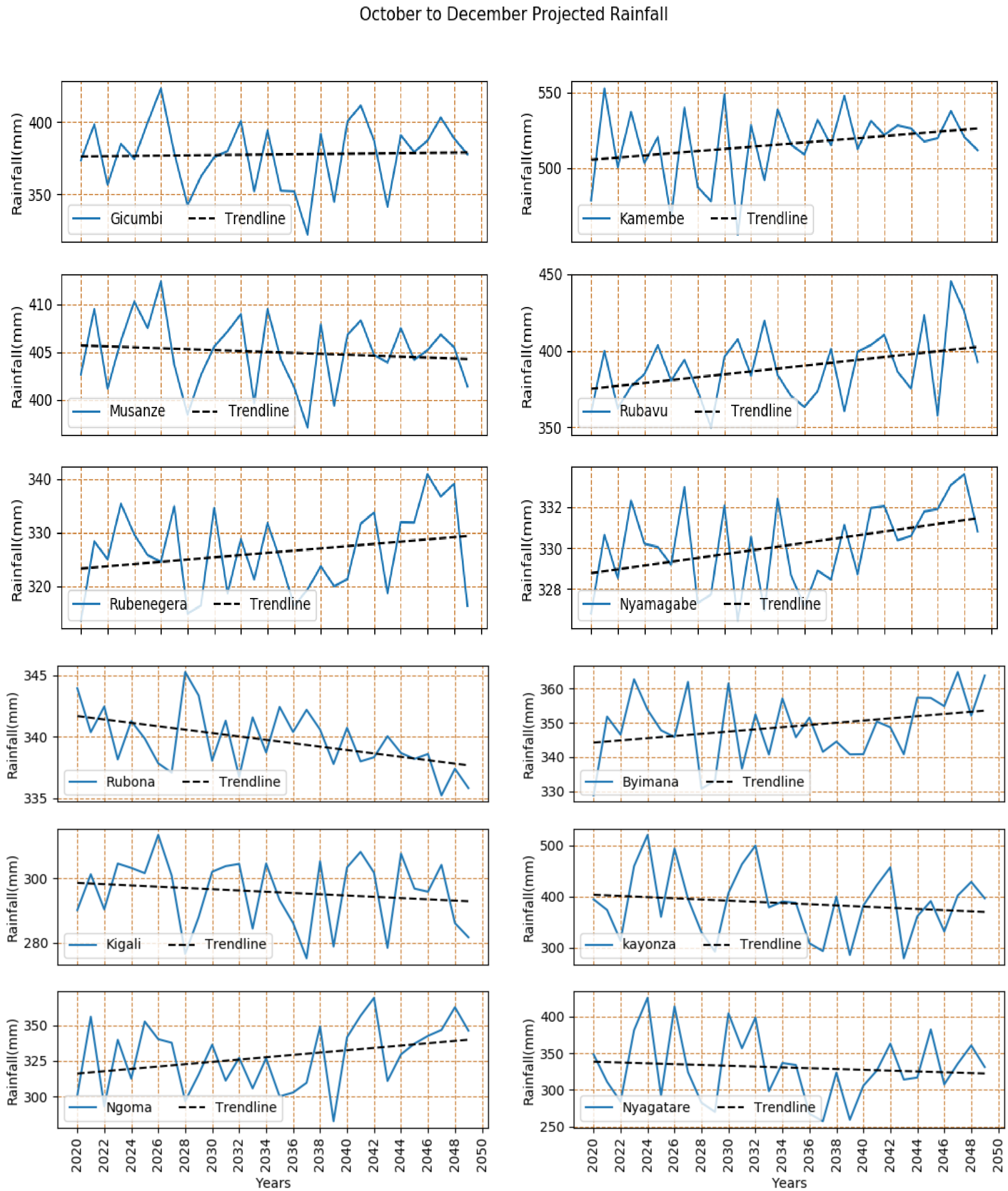

Figure 18: *Projected rainfall (2020-2049) using RCP8.5 from CCCma model during October to December rain season.*

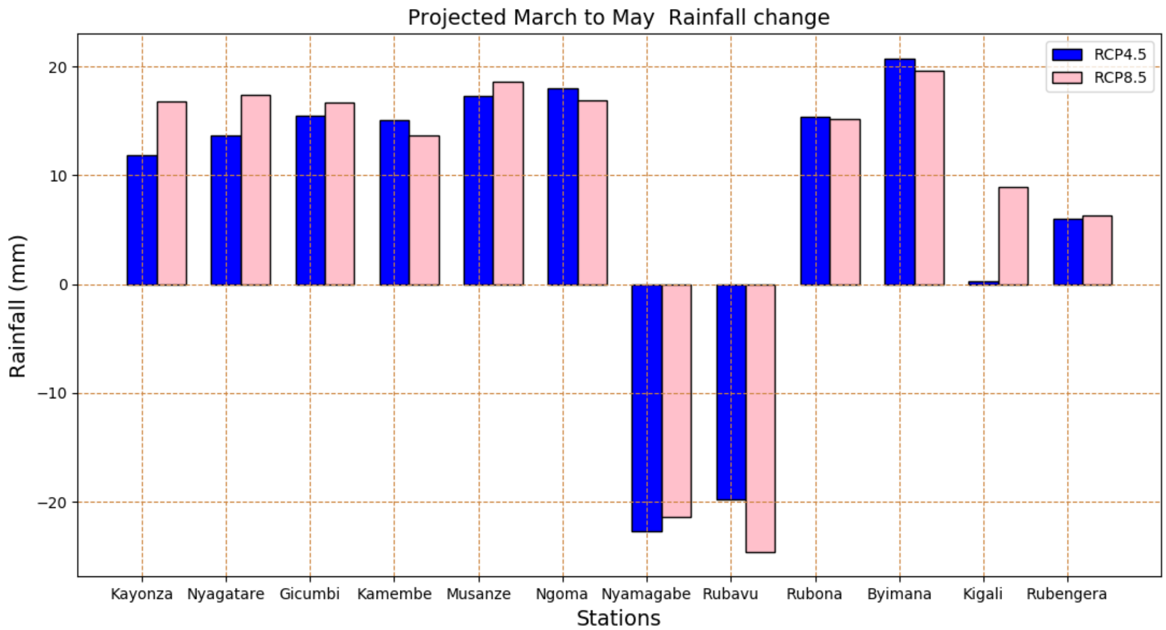

:

Figure 19: *Projected MAM rainfall change (mm) using RCP4.5 and RCP 8.5 using IPSL model 2020-2049*

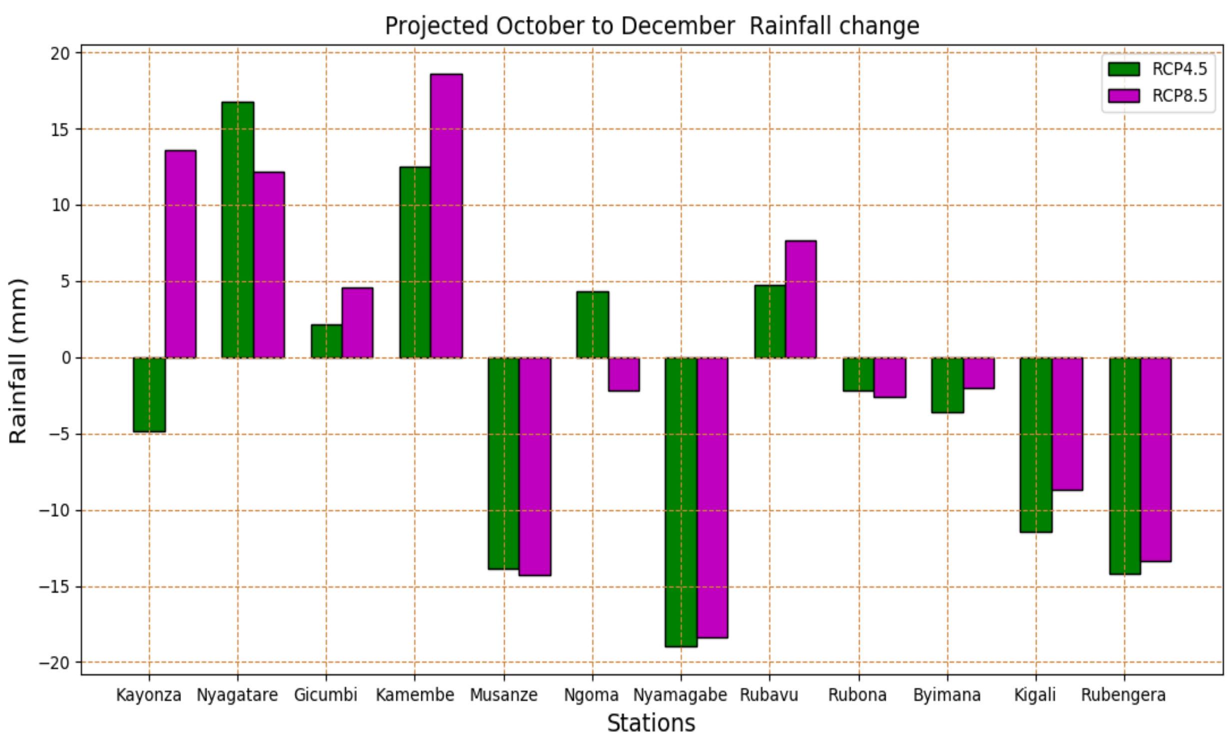

Figure 20*: Projected OND rainfall change using RCP4.5 and RCP 8.5 from CCCma model 2020-2049*

REFERENCES

[1] I. Muhire, Tesfamichael, Ahmed, and E. Minani, “Spatio-Temporal Trend Analysis of Projected Temperature over Rwanda,” *IOSR J. Environ. Sci. Ver. I,* vol. 9, no. 11, pp. 2319–2399, 2015.

[2] I. Muhire and F. Ahmed, “Spatio-temporal trend analysis of precipitation data over Rwanda,” no. June 2014, pp. 37–41.

[3] D. Ntwali, B. A. Ogwang, and V. Ongoma, “The Impacts of Topography on Spatial and Temporal Rainfall Distribution over Rwanda Based on WRF Model,” *Atmos. Clim. Sci.*, vol. 06, no. 02, pp. 145–157, 2016.

[4] MIDIMAR, “The National Risk Atlas of Rwanda,” 2015.

[5] REMA, “The assessment of economic impacts of the 2012 wet season flooding in Rwanda,” 2013.

[6] E. Nduwayezu, M. Kanevski, and M. Jaboyedoff, “Rainfall variability modelling in Rwanda,” *Geophys. Res. Abstr.*, vol. 14, no. April, p. 5569, 2012.

[7] B. Safari, “Trend Analysis of the Mean Annual Temperature in Rwanda during the Last Fifty Two Years,” *J. Environ. Prot. (Irvine,. Calif).*, vol. 03, no. 06, pp. 538–551, 2012.

[8] J. Ramirez-villegas, J. Andrew, C. M. Dunning, R. P. Allan, and E. Black, “Identification of deficiencies in seasonal rainfall simulated by CMIP5 climate models OPEN ACCESS Identification of deficiencies in seasonal rainfall simulated by CMIP5 climate models,” 2017.

[9] D. B. Lobell, M. B. Burke, C. Tebaldi, M. D. Mastrandrea, W. P. Falcon, and R. L. Naylor, “Prioritizing Climate Change Adaptation Need for Food Security in 2030,” *Science (80-.).*, vol. 319, no. February, pp. 607–610, 2008.

[10] P. Roudier, B. Sultan, P. Quirion, and A. Berg, “The impact of future climate change on West African crop yields: What does the recent literature say?,” *Glob. Environ. Chang.*, vol. 21, no. 3, pp. 1073–1083, 2011.

[11] C. Funk *et al.*, “Warming of the Indian Ocean threatens eastern and southern African food security but could be mitigated by agricultural development,” *Proc. Natl. Acad. Sci.*, vol. 105, no. 32, pp. 11081–11086, 2008.

[12] A. Challinor, T. Wheeler, C. Garforth, P. Craufurd, and A. Kassam, “Assessing the vulnerability of food crop systems in Africa to climate change.,” *Clim. Chang. 83(3), pp.381-399.*, vol. 83, no. 3, pp. 381–399, 2007.

[13] L. Ilunga, I. Muhire, and C. Mbaragijimana, “Saisons pluviométriques et origine des pluies au Rwanda,” *Geo. Eco. Trop.*, vol. 28, no. 1–2, pp. 61–68, 2004.

[14] N. J. Felix, “Characteristics of Extreme Rainfall Events,” no. August, 2015.

[15] F. Ntirenganya, “Analysis of Rainfall Data from Rwanda Analysis of Rainfall Data from Rwanda,” no. March, 2016.

[16] I. Muhire, F. Ahmed, and K. Abutaleb, “Relationships between Rwandan seasonal rainfall anomalies and ENSO events,” *Theor. Appl. Climatol.*, vol. 122, no. 1–2, pp. 271–284, 2015.

[17] S. M. Henninger, “Does the global warming modify the local Rwandan climate?,” *Nat. Sci.*, vol. 05, no. 01, pp. 124–129, 2013.

[18] L. Ilunga and I. Muhire, “Comparaison des fluctuations des précipitations moyennes annuelles au Rwanda avec les épisodes EL-NINO / LA NINA et les cycles des taches solaires,” *Geo. Eco. Trop.*, vol. 34, pp. 75–86, 2010.

[19] R. E.Okoola, “Midtropospheric Circulation Patterns Associated with Extreme Dry and Wet Episodes over Equatorial Eastern Africa during the Northern Hemisphere Spring,” *J. Appl. Meteorol.*, vol. 38, pp. 1161–1169, 1999.

[20] C. C. Mutai, W. M. Neil., and M. C. Meteorological, “East African Rainfall and the Tropical Circulation / Convection on Intraseasonal to Interannual Timescales,” *J. Clim. Clim.*, vol. 13, no. 22, pp. 3915–3939, 2000.

[21] M. Kizza, A. Rodhe, C. Xu, H. K. Ntale, and S. Halldin, “Temporal rainfall variability in the Lake Victoria Basin in East Africa during the twentieth century,” pp. 119–135, 2009.

[22] R. E. Okoola, “A diagnostic study of East African monsoon circulation during the northern hemisphere spring season,” *Int. J. Climatol.*, vol. 19, pp. 143–169, 1999.

[23] E. Koech, “Systems Associated With Wet Spells Over Kenya During The Usually Dry December-February Season,” 2014.

[24] J. N. Mutemi, “Climate anomalies over Eastern Africa associated with various ENSO Evolution phases,” 2003.

[25] P. Camberlin, “Intraseasonal Variations of June-September Rainfall and Upper-Air Circulation over Kenya,” *Theor. Appl. Climatol.*, vol. 115, pp. 107–115, 1994.

[26] W. Gitau, L. Ogallo, P. Camberlin, and R. Okoola, “Spatial coherence and potential predictability assessment of intraseasonal statistics of wet and dry spells over Equatorial Eastern Africa,” *Int. J. Climatol.*, vol. 33, no. 12, pp. 2690–2705, 2013.

[27] M. Indeje, F. H. M. Semazzi, and L. J. Ogallo, “ENSO signals in East African rainfall seasons,” *Int. J. Climatol.*, vol. 20, no. 1, pp. 19–46, 2000.

[28] S. E. Nicholson, D. Leposo, and J. Grist, “The relationship between El Niño and drought over Botswana,” *J. Clim.*, vol. 14, no. 3, pp. 323–335, 2001.

[29] M. Kienast, J. Lynch-stieglitz, L. Newman, and T. Kiefer, “El Niño-Southern Oscillation,” *Pages News*, vol. 16, no. 1, p. 300, 2008.

[30] C. J. Schreck and F. H. M. Semazzi, “Variability of the recent climate of eastern Africa,” *Int. J. Climatol.*, vol. 24, no. 6, pp. 681–701, 2004.

[31] S. Hastenrath and D. Polzin, “Dynamics of the surface wind field over the equatorial Indian Ocean,” *Q. J. R. Meteorol. Soc.*, vol. 130, no. 597, pp. 503–517, 2004.

[32] C. C. Mutai, M. N. Ward, and A. W. Colman, “Towards the prediction of the East Africa short rains based on sea-surface temperature–atmosphere coupling,” *Int. J. Climatol.*, vol. 18, no. 9, pp. 975–997, 1998.

[33] S. Edition and B. M. Glantz, “Book review,” pp. 71–74, 2001.

[34] L. J. Ogallo, “Relationships between seasonal rainfall in East Africa and the Southern Oscillation,” *J. Climatol.*, vol. 8, no. 1, pp. 31–43, 1988.

[35] L. J. Ogallo, J. E. Janowiak, and M. S. Halpert, “Teleconnection between seasonal rainfall over East Africa and global sea surface temperature anomalies,” *J. Meteorol. Soc. Japan JMSJAU*, vol. 66, no. December, pp. 807–822, 1988.

[36] M. Indeje and F. H. M. Semazzi, “Relationships Between QBO in the Lower Equatorial Stratospheric Zonal Winds and East African Seasonal Rainfall,” vol. 244, pp. 227–228, 2000.

[37] N. H. Saji and P. N. Vinayachandran, “A dipole mode in the tropical Indian Ocean,” vol. 401, no. September, pp. 360–364, 1999.

[38] C. O. Clark, P. J. Webster, and J. E. Cole, “Interdecadal variability of the relationship between the Indian Ocean zonal mode and East African coastal rainfall anomalies,” *J. Clim.*, vol. 16, no. 3, pp. 548–554, 2003.

[39] L. Ilunga, D. Mukingambeho, A. Mugwaneza, and A. Mugiraneza, “Dates probables des semailles au Rwanda Probable sowing time in Rwanda La détermination du calendrier agricole est d ’ une très grande importance dans les pays,” pp. 29–36, 2008.

[40] B. Pohl, P. Camberlin, B. Pohl, P. Camberlin, and M. Oscillation, “Influence of the Madden-Julian Oscillation on East African rainfall . Part II : March-May season extremes and interannual variability To cite this version : HAL Id : hal-00076677,” 2009.

[41] J. N. Sebaziga, “Association between madden-julian oscillations and wet and dry spells over rwanda,” p. 58, 2014.

[42] B. A. Ogwang, H. Chen, X. Li, C. Gao, T. Prof, and C. Author, “The influence of Topography on East African October to December climate : Sensitivity experiments with RegCM4 Key Laboratory of Meteorological Disaster , Ministry of Education , Nanjing University of E-mail Addresses : bob_ogwang@yahoo.co.uk (Bob Alex Og,” vol. 2014, pp. 1–27, 2014.

[43] M. F.D, I. J.M, and F. J. Opijah, “Relationship between ENSO parameters and the trends and periodic flactuations in east African rainfall.,” *J. kenya meteoroloSoc*, vol. 1, no. 1, pp. 20–43, 2007.

[44] P. Camberlin and R. E. Okoola, “The onset and cessation of the ‘“ long rains ”’ in eastern Africa and their interannual variability,” *Theor. Appl. Climatol.*, vol. 54, no. 1–2, pp. 43–54, 2003.

[45] P. Camberlin and J. G. Wairoto, “Theoretical and Applied Climatology Intraseasonal Wind Anomalies Related to Wet and Dry Spells During the ‘long’ and ‘short’ Rainy Seasons in Kenya,” *Theor. Appl. Clim.*, vol. 58, pp. 57–69, 1997.

[46] E. K. Anyamba, “On the monthly mean lower tropospheric circulation and the anomalous circulation during the 1961/62 floods in East Africa.,” no. November, 1984.

[47] Y. Sokona and F. Denton, “Climate change impacts: can Africa cope with the challenges?,” *Clim. Policy*, vol. 1, no. 1, pp. 117–123, 2001.

[48] S. Huq, H. Reid, M. Konate, A. Rahman, Y. Sokona, and F. Crick, “Mainstreaming adaptation to climate change in Least Developed Countries (LDCs),” *Clim. Policy*, vol. 4, no. 1, pp. 25–43, 2004.

[49] F. and A. O. (FAO), “Climate change and food security : A frame work document,” 2008.

[50] L. C. Stringer, D. D. Mkwambisi, A. J. Dougill, and J. C. Dyer, “Adaptation to climate change and desertification: Perspectives from national policy and autonomous practice in Malawi,” *Clim. Dev.*, vol. 2, no. 2, pp. 145–160, 2010.

[51] M. Niasse, A. Afouda, and A. Amani, “Reducing West Africa’s Vulnerability to Climate Impacts on Water Resources , Wetlands and Desertification: Elements for a Regional Strategy for Preparedness and Adaptation,” *World*, pp. 1–16, 2004.

[52] H. Gharbi, M. Massaoudi, S. Bahroun, and E. Zagrouba, “Key frames extraction based on local features for efficient video summarization,” *Lect. Notes Comput. Sci. (including Subser. Lect. Notes Artif. Intell. Lect. Notes Bioinformatics)*, vol. 10016 LNCS, pp. 275–285, 2016.

[53] C. Ringler, T. Zhu, X. Cai, J. Koo, D. Wang, and IFRI, “Climate Change Impacts on Food Security in Sub-Saharan Africa Insights from Comprehensive Climate Change Scenarios,” *Food Policy*, vol. 466, no. December, p. 28, 2010.

[54] K. S. Ndlovu, “An evaluation of East African rainfall variability in the EC-Earth ensemble of simulations for CMIP5 Kgololesego Sally Ndlovu July 2013 A dissertation submitted for the degree of MSc in Atmospheric Sciences , Oceanography and Climate,” no. July, pp. 1–69, 2013.

[55] B. Nyenzi, “Mechanisms of East African Rainfall variability,” no. July, p. 184, 1988.

[56] Z. Owiti, “Linkages between the Indian Ocean Dipole and East African Seasonal Rainfall Anomalies National Council for Science and Technology IGAD Climate Prediction and Applications Centre,” vol. 2, no. April, pp. 3–17, 2008.

[57] O. Peter., O. Laban., O. Raphael., H. Herry., and W. Mathewe., “East African Rainfall Variability Associated with the Madden-Julian Oscillation,” *J. Kenya Meteorol. Soc.*, vol. 2, no. October, pp. 105–114, 2008.

[58] R. A. Madden and P. R. Julian, “Observations of the 40–50-Day Tropical Oscillation—A Review,” *Monthly Weather Review*, vol. 122, no. 5. pp. 814–837, 1994.

[59] M. E. Shongwe, G. J. van Oldenborgh, B. J. J. M. van den Hurk, B. de Boer, C. A. S. Coelho, and M. K. van Aalst, “Projected Changes in Mean and Extreme Precipitation in Africa under Global Warming. Part I: Southern Africa,” *J. Clim.*, vol. 22, no. 13, pp. 3819–3837, 2009.

[60] J. Gasore and B. S. Physics, “Quantifying Emissions of Carbon Dioxide and Methane in Central and Eastern Africa Through High Frequency Measurements and Inverse Modeling,” 2018.

[61] IPCC, “Climate Change 2014 Synthesis Report Summary Chapter for Policymakers,” *Ipcc*, p. 31, 2014.

[62] A. Jarvis, J. R. Ramirez-Villegas, B. V Herrera Campo, and C. Navarro-Racines, “Is Cassava the Answer to African Climate Change Adaptation?,” *Trop. Plant Biol.*, vol. 5, no. 1, pp. 9–29, 2012.

[63] P. G. Jones and P. K. Thornton, “The potential impacts of climate change on maize production in Africa and Latin America in 2055,” *Glob. Environ. Chang.*, vol. 13, no. 1, pp. 51–59, 2003.

[64] M. Boko *et al.*, “Africa ,Climate change 2007: Impacts, adaptation and vulnerability. Contribution of Working Group II to the Fourth Assessment Report of the Intergovernmental Panel on Climate Change,” *Clim. Chang. 2007 Impacts, Adapt. vulnerability. Contrib. Work. Gr. II to Fourth Assess. Rep. Intergov. Panel Clim. Chang.*, pp. 433–467, 2008.

[65] C. Sabine, “The IPCC fifth assessment report,” *Carbon Manag.*, vol. 5, no. 1, pp. 17–25, 2014.

[66] R. L. Wilby, S. P. Charles, E. Zorita, B. Timbal, P. Whetton, and L. O. Mearns, “Guidelines for Use of Climate Scenarios Developed from Statistical Downscaling Methods,” *Analysis*, vol. 27, no. August, pp. 1–27, 2004.

[67] X. C. Zhang, “CLIGEN non-precipitation parameters and their impact on WEPP crop simulation,” *Appl. Eng. Agric.*, vol. 20, no. 4, pp. 447–454, 2004.

[68] J. Trotochaud, “Climate change impact assessments using the Water Erosion Prediction Project model,” 2015.

[69] S. Trzaska and E. Schnarr, “A review of downscaling methods for climate change projections,” *United States Agency Int. Dev. by Tetra Tech ARD*, no. September, pp. 1–42, 2014.

[70] S. N. Ngigi, H. H. G. Savenije, J. Rockström, and C. K. Gachene, “Hydro-economic evaluation of rainwater harvesting and management technologies: Farmers’ investment options and risks in semi-arid Laikipia district of Kenya,” *Phys. Chem. Earth*, vol. 30, no. 11–16 SPEC. ISS., pp. 772–782, 2005.

[71] E. Zorita and H. von Storch, “The analog method as a simple statistical downscaling technique:comparison with more complicated methods,” *J. Clim.*, vol. 12, pp. 2474–2489, 1999.

[72] H. S. Endris *et al.*, “Assessment of the performance of CORDEX regional climate models in simulating East African rainfall,” *J. Clim.*, vol. 26, no. 21, pp. 8453–8475, 2013.

[73] B. Lyon and N. Vigaud, “Unraveling East Africa ’ s Climate Paradox,” pp. 265–281, 2017.

[74] M. Glotter, J. Elliott, D. McInerney, N. Best, I. Foster, and E. J. Moyer, “Evaluating the utility of dynamical downscaling in agricultural impacts projections,” *Proc. Natl. Acad. Sci.*, vol. 111, no. 24, pp. 8776–8781, 2014.

[75] P. Luhunga, J. Botai, and F. Kahimba, “Evaluation of the performance of CORDEX regional climate models in simulating present climate conditions of Tanzania Evaluation of the performance of CORDEX regional climate models in simulating present climate conditions of Tanzania,” *J. South. Hemisph. Earth Syst. Sci.*, vol. 66, no. March, pp. 32–54, 2016.

[76] E. Mutayoba and J. J. Kashaigili, “Evaluation for the Performance of the CORDEX Regional Climate Models in Simulating Rainfall Characteristics over Mbarali River Catchment in the Rufiji Basin, Tanzania,” *J. Geosci. Environ. Prot.*, vol. 05, no. 04, pp. 139–151, 2017.

[77] M. E. Shongwe, C. Lennard, B. Liebmann, E.-A. Kalognomou, L. Ntsangwane, and I. Pinto, “An evaluation of CORDEX regional climate models in simulating precipitation over Southern Africa,” *Atmos. Sci. Lett.*, vol. 16, no. 3, pp. 199–207, 2015.

[78] C. C. Funk and M. E. Brown, “Intra-seasonal NDVI change projections in semi-arid Africa,” *Remote Sens. Environ.*, vol. 101, no. 2, pp. 249–256, 2006.

[79] V. Ongoma, H. Chen, and C. Gao, “Projected changes in mean rainfall and temperature over East Africa based on CMIP5 models,” *Int. J. Climatol.*, 2017.

[80] T. C. Fotso-nguemo, “Projected trends of extreme rainfall events from CMIP5 models over Central Africa,” no. January, pp. 1–8, 2018.

[81] L. Ogallo, “Trend of rainfall in East Africa,” pp. 83–90, 1981.

[82] J. Hamisi, “Study of Rainfall Trends and Variability Over Tanzania,” no. August, p. 55, 2013.

[83] G. C. Blain, “The Mann-Kendall test: the need to consider the interaction between serial correlation and trend - doi: 10.4025/actasciagron.v35i4.16006,” *Acta Sci. Agron.*, vol. 35, no. 4, pp. 393–402, 2013.

[84] K. Drapela and I. Drapelova, “Application of Mann-Kendall test and the Sen’s slope estimates for trend detection in deposition data from Bily Kriz (Beskydy Mts., the Czech Republic) 1997--2010,” *Beskydy*, vol. 4, no. 2, pp. 133–146, 2011.

[85] M. G. Kendall, “Appendix: Mann-Kendall Trend Tests,” *Oxford Univ. Press*, p. 202, 1975.

[86] V. Ongoma, J. N. Muthama, and W. Gitau, “Evaluation of urbanization on urban temperare of Nairobi City, Kenya,” *Glob. Meteorol.*, vol. 2, no. e1, pp. 1–5, 2013.

[87] F. W. Nsubuga, J. M. Olwoch, and H. Rautenbach, “Variability properties of daily and monthly observed near-surface temperatures in Uganda: 1960-2008,” *Int. J. Climatol.*, vol. 34, no. 2, pp. 303–314, 2014.

[88] V. Ongoma and H. Chen, “Temporal and spatial variability of temperature and precipitation over East Africa from 1951 to 2010 Temporal and spatial variability of temperature and precipitation over East Africa from 1951 to 2010,” *Meteorol. Atmos. Phys.*, vol. 129, no. 2, pp. 131–144, 2017.

[89] H. Theil, “A rank-invariant method of linear and polynomial regresion analysis, II,” *Ned. Akad. Wetensch. Proc.*, vol. 53, pp. 521–525, 1950.

[90] P. K. Sen, “Estimates of the Regression Coefficient Based on Kendall’s Tau,” *J. Am. Stat. Assoc.*, vol. 63, no. 324, pp. 1379–1389, 1968.

[91] C. J. Willmott *et al.*, “Statistics for the evaluation and comparison of models,” *J. Geophys. Res. Ocean.*, vol. 90, no. C5, pp. 8995–9005, 1985.

[92] E. A. Kalognomou *et al.*, “A diagnostic evaluation of precipitation in CORDEX models over Southern Africa,” *J. Clim.*, vol. 26, no. 23, pp. 9477–9506, 2013.

[93] George H. Hargreaves and Zohrab A. Samani, “Reference Crop Evapotranspiration from Temperature,” *Appl. Eng. Agric.*, vol. 1, no. 2, pp. 96–99, 1985.

[94] C. J. Willmott and K. Matsuura, “Advantages of the mean absolute error (MAE) over the root mean square error (RMSE) in assessing average model performance,” *Clim. Res.*, vol. 30, no. 1, pp. 79–82, 2005.

[95] C. J. Willmott and K. Matsuura, “On the use of dimensioned measures of error to evaluate the performance of spatial interpolators,” *Int. J. Geogr. Inf. Sci.*, vol. 20, no. 1, pp. 89–102, 2006.

[96] T. Chai and R. R. Draxler, “Root mean square error (RMSE) or mean absolute error (MAE)? -Arguments against avoiding RMSE in the literature,” *Geosci. Model Dev.*, vol. 7, no. 3, pp. 1247–1250, 2014.

[97] M. H. Omondi, “Assessment of temperature and precipitation extremes over kenya using the coordinated regional downscaling experiment model outputs. MSc Thesis. July, 2015".

[98] S. Chatterjee and A. S. Hadi, “Simple linear regression,” *Regres. Anal. by Ex.*, no. April, pp. 21–51, 2012.

[99] W. J. Boscardin, “The Use and Interpretation of Linear Regression Analysis in Ophthalmology Research,” *Am. J. Ophthalmol.*, vol. 150, no. 1, pp. 1–2, 2010.

[100] H. Mohammed, C. K. Jean, and W. A. Ahmad, “Projections of precipitation, air temperature and potential evapotranspiration in Rwanda under changing climate conditions,” *African J. Environ. Sci. Technol.*, vol. 10, no. 1, pp. 18–33, 2016.

[101] A. P. Williams and C. Funk, “A westward extension of the warm pool leads to a westward extension of the Walker circulation, drying eastern Africa,” *Clim. Dyn.*, vol. 37, no. 11–12, pp. 2417–2435, 2011.

[102] B. Lyon and D. G. Dewitt, “A recent and abrupt decline in the East African long rains,” *Geophys. Res. Lett.*, vol. 39, no. 2, pp. 1–5, 2012.

[103] W. Yang, R. Seager, M. A. Cane, and B. Lyon, “The East African Long Rains in Observations and Models Wenchang Yang Bradfield Lyon,” pp. 1–42, 2014.

[104] J. E. Tierney, J. E. Smerdon, K. J. Anchukaitis, and R. Seager, “Multidecadal variability in East African hydroclimate controlled by the Indian Ocean,” *Nature*, vol. 493, no. 7432, pp. 389–392, 2013.

[105] C. C. Ummenhofer, A. Sen Gupta, M. H. England, and C. J. C. Reason, “Contributions of Indian Ocean sea surface temperatures to enhanced East African rainfall,” *J. Clim.*, vol. 22, no. 4, pp. 993–1013, 2009.

[106] A. M. Thomson *et al.*, “RCP4.5: A pathway for stabilization of radiative forcing by 2100,” *Clim. Change*, vol. 109, no. 1, pp. 77–94, 2011.

[107] G. P. Wayne, “The Beginner’s Guide to Representative Concentration Pathways (RCPs),” *Skept. Sciece*, vol. 1.0, pp. 1–24, 2013.

[108] M. Meinshausen *et al.*, “The RCP greenhouse gas concentrations and their extensions from 1765 to 2300,” *Clim. Change*, vol. 109, no. 1, pp. 213–241, 2011.

[109] J. Rogelj, M. Meinshausen, and R. Knutti, “Global warming under old and new scenarios using IPCC climate sensitivity range estimates,” *Nat. Clim. Chang.*, vol. 2, no. 4, pp. 248–253, 2012.

[110] J. F. Lamarque *et al.*, “Global and regional evolution of short-lived radiatively-active gases and aerosols in the Representative Concentration Pathways,” *Clim. Change*, vol. 109, no. 1, pp. 191–212, 2011.